Title
SUPERCONDUCTIVE BOLOMETERS FOR SUBMILLIMETER WAVELENGTHS

Author
Clarke, J.

Publication Date
1977-04-01

Submitted to Journal of Applied Physics

LBL-5766
Preprint

SUPERCONDUCTIVE BOLOMETERS FOR SUBMILLIMETER WAVELENGTHS

J. Clarke, G. I. Hoffer, P. L. Richards, and N.-H. Yeh

April 1977

Prepared for the U. S. Energy Research and Development Administration under Contract W-7405-ENG-48

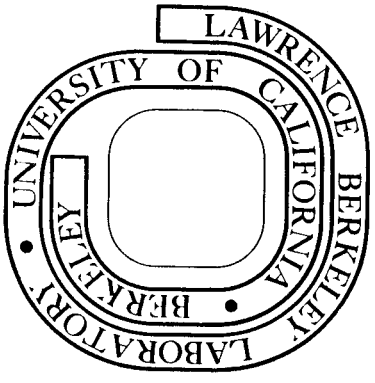

DISCLAIMER

To be submitted to J. Appl. Phys. LBL-5766

SUPERCONDUCTIVE BOLOMETERS FOR SUBMILLIMETER WAVELENGTHS†

J. Clarke, G. I. Hoffer, P. L. Richards, and N.-H. Yeh

Department of Physics, University of California
and Materials and Molecular Research Division
Lawrence Berkeley Laboratory
Berkeley, California 94720

ABSTRACT

Three types of composite superconductive bolometer are described in which the temperature sensitive element is a superconducting film at the transition temperature, a superconductor-normal metal-superconductor Josephson junction, or a superconductor-insulator-normal metal quasiparticle tunneling junction. The temperature sensitive element is evaporated onto a sapphire substrate on the reverse side of which is a bismuth film to absorb the submillimeter radiation. The noise limitations of each type of bolometer are calculated. The fabrication and measured performance of the transition edge bolometer and the Josephson junction bolometer are described. The best electrical NEP obtained with a transition edge bolometer fabricated on a 4 × 4 × 0.005 mm sapphire substrate, is $(1.7 \pm 0.1) \times 10^{-15}$ WHz$^{-\frac{1}{2}}$ at 2 Hz at an operating temperature of 1.27 K. This NEP is within a factor 2 of the thermal noise limit. The effective absorptivity of the bismuth film is measured to be 0.47 ± 0.05, and the corresponding detectivity, D*, is calculated to be $(1.1 \pm 0.1) \times 10^{14}$ cm W^{-1} Hz$^{\frac{1}{2}}$. Suggestions are made for further improvements in sensitivity.

1. INTRODUCTION

The germanium bolometer developed by Low[1] has been the most widely used broadband detector for slowly varying signals at infrared wavelengths $\lambda \gtrsim 100$ μm where well developed photoconductors are not yet available. The power which must be dissipated in the bolometer to produce a signal equal to the rms noise (often called the electrical noise-equivalent-power or NEP) can approach $10^{-15}\,\mathrm{WHz}^{-\frac{1}{2}}$ for small ($\lesssim 3 \times 10^{-2}$ mm^3) bolometers optimized for operation at pumped ^{4}He temperatures on a low background environment. The optical NEP (the optical power incident in the geometrical bolometer area required to produce a signal equal to the rms noise) is given by the electrical NEP divided by an optical efficiency factor ε. The bolometer area required for efficient coupling to a signal containing n modes increases with wavelength approximately as $n\lambda^2$. Since the optical extinction lengths of many absorbing materials (including black paints and semiconductors which are appropriately doped for bolometric applications) increase with λ in this wavelength region, the bolometer thickness must

also increase with λ for good optical efficiency. The electrical NEP of a bolometer optimized for a specified modulation frequency in a low background environment varies as the square root of the heat capacity. Therefore, bolometers used at submillimeter wavelengths have typically shown poor sensitivity because of poor optical efficiency and/or large electrical NEP. We have developed a composite absorbing structure for use in submillimeter bolometers. This structure consists of a thin metallic film absorber ($\sim$ 200 $\Omega/\square$ of Bi) on the reverse side of a low heat capacity dielectric substrate (sapphire or diamond). An absorber of this general class is well known to infrared technology from its use in the Golay cell, but apparently had not previously been used in bolometers. A theoretical and experimental analysis is presented in Section 6 which shows that a broadband absorptivity of $\sim$ 50% is available in a single pass. An absorptivity approaching 100% is obtainable at selected wavelengths.

Composite structures of different types have been used by other workers to improve optical efficiency. These include the use of black paint to reduce the dielectric reflectivity of semiconducting bolometers[1], the use of black paint on a metal foil to extend the bolometer area[2], and the use of a resonant slice of doped Si attached to a small Ge thermometer to make a large area bolometer that is efficient in one or more narrow wavelength bands[3]. Only in the last mentioned case is the combination of heat capacity per unit area and absorptivity in the submillimeter band competitive with the structures described in this paper.

In order to make a bolometer from such an absorbing element, it is necessary to attach a sensitive thermometer and to provide electrical

and thermal contact as well as mechanical support while maintaining the lowest possible heat capacity. One approach is to glue a small doped Ge thermometer to the absorber, and to provide electrical and thermal contact via the wire leads to the thermometer. This approach was first used by the Caltech group[4], and has subsequently been extensively developed at Berkeley[5]. In large area bolometers, it has proved desirable to add nylon threads for supplementary mechanical support to minimize microphonic noise. Bolometers made in this way have proved very useful for submillimeter wave astronomy and laboratory experiments, but they are not optimum in two important respects. First, the combination of wire, solder, Ge, and glue used for the thermometer typically makes a significant contribution to the heat capacity of the bolometer. Second, these thermometers generate noise with an inverse frequency spectral density that is proportional to the square of the bias current. The effects of this noise on bolometer performance are considered elsewhere[5].

We have explored the use of evaporated film superconductive thermometers for our composite bolometer structure. They are easy to attach to the substrate, and have low heat capacity and high sensitivity. The idea of using the large temperature coefficient of resistance of a superconductor operated at its transition temperature for the thermometric element of a bolometer is an old one[6]. These bolometers have not been competitive in low frequency applications, however, because of excessive low frequency noise. Recently, the work of Clarke, Voss[7], Hsiang[8], and Hawkins[9] has shown that this noise arises from thermal fluctuations in the metal film, and that by suitable procedures it can be made comparable with or less than Johnson noise.

We have investigated three types of superconductive thermometers. The transition edge bolometer mentioned above appears to be the most promising at the present time. For operation at pumped ^{4}He temperatures we use an aluminum film with a transition temperature in the range from 1.2 to 1.4 K, and with a normal state resistance of a few ohms. For optimum system performance, it is necessary to provide a readout system with a noise temperature $T_N \lesssim 1$ K at a frequency of a few Hz. This performance can be achieved by using an ac bolometer bias current to avoid low frequency amplifier noise, and a cooled transformer that steps up the bolometer resistance to a value that is optimum for the preamplifier.

A second type of superconductive bolometer makes use of the temperature dependence of the critical current of a superconductor-normal metal-superconductor (SNS) Josephson tunnel junction[10]. Since the impedance of such junctions is $\sim 10^{-6}$ Ω, a Superconducting QUantum Interference Device[11] (SQUID) is used as a first stage amplifier with $T_N < 1$ K. This bolometer performs comparably to the transition edge bolometer, but is more complex and generally more difficult to fabricate and use. Consequently, the transition edge bolometer is the more practical for most purposes.

We also considered a third type of superconductive bolometer, which uses the temperature-dependent quasiparticle-tunneling resistance of a superconductor-insulator-normal metal (SIN) tunnel junction[12]. The theoretical sensitivity of such a bolometer is comparable with that of the transition edge and SNS bolometers. For use as a thermometer, however, the SIN junction must have a sufficiently small (temperature independent) leakage current. We were not able to fabricate junctions with the required

electrical properties which also had the required long term stability over many thermal cycles. We have not operated bolometers of this type.

In this paper, we discuss the design, optimization, and fabrication of transition edge and SNS superconductive composite bolometers. A short theoretical discussion of the SIN bolometer is included for completeness. Although comparable performance can be expected from all three types of bolometer, the essential simplicity of the transition edge thermometer makes it more attractive at present. This type of bolometer has been developed more thoroughly and consequently shows the best experimental performance. We have measured an electrical NEP of $(1.7 \pm 0.1) \times 10^{-15}$ WHz$^{-\frac{1}{2}}$ at 2 Hz in a large area (4 × 4 mm) ^{4}He temperature bolometer operated in a low background environment with a time constant of 8×10^{-2} s. This electrical NEP is within a factor 2 of the thermal noise limit and is at least as good as the best small Ge bolometers at the same temperature. It would be improved somewhat by the use of a lower heat capacity diamond substrate.

We further describe measurements of the submillimeter wave absorptivity of Bi coated sapphire substrates, and of the optical efficiency of completed bolometers. The theoretical prediction of 50 percent optical efficiency for a bolometer designed for broadband applications has been verified experimentally for frequencies in the vicinity of 20 cm^{-1}. Because of their large area and relatively high optical efficiency, the specific detectivity $D^* = \&_e (\text{Area})^{\frac{1}{2}}/\text{NEP} = (1.1 \pm 0.1) \times 10^{14}$ cm W^{-1} Hz$^{\frac{1}{2}}$ of our best bolometer is the largest ever measured for a submillimeter wave detector ($\&_e$ is the effective absorptivity of the bolometer).

Preliminary reports of our development of composite superconducting bolometers have appeared elsewhere[13,14].

2. BOLOMETER THEORY

Consider a bolometer with heat capacity C at temperature T connected to a heat sink at temperature T_s via a thermal conductance G. The thermal time constant, τ, is C/G. In the case of a composite bolometer, the substrate absorbs a fraction $\varepsilon(\leq 1)$ of the incident signal power, P_s, and the resulting increase in temperature is detected by a separate temperature-sensitive element (thermometer) attached to the substrate. This element is biased with a constant current I that generates a voltage V across it. If the signal is chopped at a frequency $\omega/2\pi$, the responsivity $S(\omega)$ is given by[15]

$$S \equiv \frac{\partial V}{\partial P_s} = \frac{\varepsilon \partial V/\partial T}{G - I\partial V/\partial T + i\omega C} = \frac{\varepsilon \partial V/\partial T}{G_e(1 + i\omega\tau_e)} \quad . \tag{2.1}$$

In Eq. (2.1), $G_e = (G - I\partial V/\partial T)$ is the effective thermal conductivity, and $\tau_e = C/G_e$ is the effective thermal time constant. To avoid thermal runaway of the bolometer, we require $G_e > 0$. If $\partial V/\partial T < 0$ (negative thermal feedback), G_e is always positive, whereas if $\partial V/\partial T > 0$ (positive thermal feedback), the bias current must satisfy the condition $I < G/(\partial V/\partial T)$.

The square of the electrical NEP (per unit bandwidth) can be written as the sum of squares of statisticaly independent terms which arise from a number of sources[15]:

$$(NEP)^2 = 8k_B T_B \varepsilon P_B + 4k_B T^2 G + J_{1/f}(f)/|S|^2 + 4k_B TR/|S|^2 + J_A(f)/|S|^2 + (NEP)_M^2 \quad . \tag{2.2}$$

The first term arises from fluctuations in the background blackbody power εP_B absorbed by the bolometer. We assume that the background temperature $T_B >> T$,

and that cooled filters are used which limit the background power to wavelengths $\lambda > hc/k_B T_B$ where the Rayleigh-Jeans limit is valid. The second term arises from the random exchange of energy between the bolometer and the heat sink via the thermal conductance. No treatment has been given of the fluctuations of a bolometer using correct non-equilibrium thermodynamics in the presence of thermal feedback. Consequently we have used in Eq. (2.2) the conventional approximate expressions derived from equilibrium thermodynamics. The third term arises from voltage noise in the thermometer which has an 1/f spectral density $J_{1/f}(f)$. The fourth term is the contribution of Johnson noise in the thermometer which has a resistance R. This term is slightly modified for a Josephson junction (see Section 4.3). The fifth term is the contribution of the amplifier that detects voltage changes across the thermometer. Here, $J_A(f)$ is the spectral density of the amplifier voltage noise. The last term is from miscellaneous sources, such as temperature fluctuations in the helium bath, microphony of the bolometer, and pick-up from radio and television stations. One attempts to reduce the noise from these sources to a level below that of the first or second term.

If the resistance of the bolometer is measured with an ac bias current and the ac voltage is subsequently lock-in amplified, additional numerical factors are introduced into Eq. (2.2). The first three terms arise from resistance fluctuations in the thermometer, and are treated by the detection system in exactly the same way as the signal. On the other hand, the fourth and fifth noise sources do not involve resistance fluctuations, and are treated differently by the lock-in amplifier. A proper consideration[16] of the lock-in amplification shows that the $(NEP)^2$ due to Johnson noise and amplifier noise should be increased by a factor of 2. Depending on their origin, the miscellaneous noise contributions to the $(NEP)^2$ may or may not contain this factor. Eq. (2.2) also reveals

that the background and thermal fluctuation $(NEP)^2$ (first and second terms) are independent of the value of $\omega\tau_e$. However, the third, fourth, and fifth terms are proportional to $(1 + \omega^2\tau_e^2)$, and therefore increase as ω^2 for frequencies higher than $1/2\pi\tau_e$.

We may draw several general conclusions about the optimization of bolometers from the form of Eqs. (2.1) and (2.2). First, the temperature T_s of the heat sink should be as low as possible. The lower limit is usually fixed by the type of cryostat used. The rapid dependence of important bolometer parameters such as R and C on temperature suggests that the operating temperature of an optimized bolometer will be confined to a small range above T_s. The operating temperature is further restricted in the case of the transition-edge bolometer by the transition temperature of available superconductors. The temperature rise of the bolometer is $T - T_s = (\varepsilon P_B + IV)/G$. For bolometer applications in which the absorbed background power εP_B is large, the value of G required to keep the bolometer cold can be sufficiently large that $G >> \omega C$. In this limit, C does not appear in Eq. (2.1) or (2.2). In the low background limit, on the other hand, C should be made as small as possible. The value of τ_e is chosen after considering the requirements of the experiment, and G_e is then equal to C/τ_e. In this limit, the bolometer NEP varies as $C^{\frac{1}{2}}$. This dependence is immediately clear if the NEP is limited by thermal fluctuation noise (the second term in Eq. (2.2)). It is also true if the NEP is limited by any of the subsequent terms in Eq. (2.2) which vary as $|S|^{-2} \propto G^2/I(\partial R/\partial T)$. Since the largest useful values of I are limited by bolometer heating to $I \approx G(T - T_s)/V$, we see that the optimum $|S|^{-2} \propto G$. Although the bolometers described in this paper are of value in both high background and low background limits, bolometers were constructed only with parameters optimized for low background applications.

3. SUPERCONDUCTING TRANSITION EDGE BOLOMETER

3.1 Principles of Operation

The transition-edge bolometer consists of a thin film of superconductor (aluminum in the present work) evaporated onto a suitable substrate. The temperature of the bolometer is maintained close to the mid-point of the superconducting transition where the resistance R of the film increases rapidly with increasing temperature. An ac current of rms amplitude I is passed through the film so that changes in temperature generate changes in the ac voltage that are detected by a low noise amplifier. The electrical responsivity is then given from Eq. (2.1) as $S = I(\partial R/\partial T)/G_e(1 + i\omega\tau_e)$. The responsivity increases with increasing bias current but, since the thermal feedback is positive, I^2 must be less than $G/(\partial R/\partial T)$. If we take as typical values $G = 5 \times 10^{-8}$ WK^{-1} and $\partial R/\partial T = 10^3$ ΩK^{-1}, this requirement implies that $I < 7$ μA. For example, if we choose $I = 1$ μA, $S \approx 2 \times 10^4$ VW^{-1} at zero frequency.

3.2 Experimental Details

The bolometers were fabricated on single-crystal sapphire substrates with dimensions 4×4×0.135 mm, 4×4×0.050 mm, or 4×2×0.135 mm (see Fig. 1). Four rectangles of In of size 0.7 × 0.15 × 0.0005 mm were evaporated onto the corners of the substrate, followed by 5 nm of Cu. (The thin Cu layer appears to stabilize the In-Al interface and to inhibit the growth of an oxide layer.) An Al strip 0.25 mm wide and 50 nm to 150 nm thick (the superconducting thermometer) was evaporated at a pressure of $\sim 2 \times 10^{-7}$ Torr

and a rate of $\sim$ 20 nm s^{-1} near one edge of the substrate, and a Bi strip 0.5 mm wide and 0.1 μm thick (the heater) was evaporated near the opposing edge. Each end of the strips made good electrical contact with an In/Cu rectangle. The edges of the Al strip were cut with a diamond knife to reduce the width of the superconducting transition[17]. The transition width was typically 3 mK. The transition temperature of the films varied from $\sim$ 1.2 K for the thicker samples to $\sim$ 1.4 K for the thinner samples. At low temperatures, the resistance of a 50 nm thick Al film in the normal state was 2 to 4 Ω, while the resistance of the Bi film was about 1500 Ω.

Four small pieces of lead foil were attached with epoxy to an OFHC copper mount as shown in Fig. 1. (OFHC copper was used to minimize the thermal equilibration time of the mount.) The epoxy provided electrical insulation between the foils and the mount. Nylon threads with a diameter of $\sim$ 15 μm were separated from a multifilament thread, and cleaned with trichloroethylene. Two threads were attached to the lead foils with GE 7031 varnish as shown. An indium film about 2 μm thick was evaporated on the In/Cu rectangles on the substrate and on the corresponding positions on the nylon threads. The substrate was then carefully pressed onto the threads so that the indium films were cold-welded together. We found that this assembly technique was highly reliable, and that the bolometer could be thermally cycled repeatly with no tendency for the nylon threads to become detached. The remaining portions of the threads were coated with 0.75 μm of indium to provide thermal and superconducting electrical connections to the thermometer and heater. This thickness gave a thermal conductance of about 5×10^{-8} WK^{-1} at the operating temper-

ature of the bolometer. A 0.08 μm bismuth film was evaporated on the back of the substrate as a far infrared absorber.

The mount was suspended from the top-plate of a vacuum can by four 1-72 nylon screws about 10 mm long. Below the mount was attached a block of copper (volume $\sim 5 \times 10^3$ mm^3) on which was wound a 1 kΩ manganin heater. This arrangement provided a low-pass thermal filter to reduce the effects of temperature fluctuations in the helium bath. The thermal time-constant of the block and bolometer mount was about 20 s. A vacuum-tight sapphire window was sealed into the top-plate of the vacuum can above the bolometer. A stainless steel light-pipe with an i.d. of about 12 mm connected the sapphire window to the top of the cryostat. The light-pipe was closed at the top with a black polyethylene sheet 200 μm thick. The vacuum can was evacuated through a 3 mm stainless steel tube that contained a radiation baffle. Leads from the bolometer circuit were brought out through a vacuum seal in the top-plate.

The Al strip formed one arm of a Wheatstone bridge, each of the other three arms being a manganin wire resistor (see Fig. 2). The bridge was operated at 1 kHz. The output voltage from the bridge was amplified by a Triad G-4 transformer with a turns ratio of 1:350. The μ-metal can had been removed from the transformer which was mounted, together with the manganin resistors, outside the vacuum can. The output of the transformer was connected to a room-temperature FET preamplifier. The cooled transformer-preamplifier combination achieves a noise temperature of about 1 K[18]. The preamplifier had a gain of 10^4 and was followed by a tuned amplifier, and a lock-in detector referenced to the 1 kHz oscillator. The output from the lock-in was available via a 1 kHz

notch-filter, and was also connected to a feedback circuit that regulated the temperature of the bolometer.

It is, of course, essential that the Al strip be maintained on the superconducting transition. Both the temperature of the helium bath and the level of the background radiation contain drifts and low frequency fluctuations (whose spectral densities vary approximately as $1/f^2$ at low frequencies) sufficiently large to drive the temperature of the bolometer well away from the transition temperature in the absence of temperature regulation. The temperature of the bolometer was regulated by feedback through an amplifier that fed current into the manganin heater on the copper block. In operation, the temperature of the helium bath was about 1.1 K, at least 0.1 K below the transition temperature of the Al. The feedback circuit supplied the appropriate current to the heater to raise the temperature of the bolometer until the resistance of the Al strip was 1 Ω. The response of the feedback circuit was small at the modulation frequency ($\gtrsim$ 1 Hz) so the amplified signal at the modulation frequency was available at the output. A slow drift in the temperature of the helium bath or in the amount of background power, on the other hand, was compensated so as to keep the bolometer at its operating temperature.

Typically, τ is 10^{-2} to 10^{-1} s, and the time constant of the copper mount, τ_m, is $\sim$ 20 s. Thus, $\tau \ll \tau_m$. Let α be the loop gain of the feedback system, typically 50. Consider fluctuations $\Delta P_B \cos(\omega t + \delta_1)$

in the background radiation and $\Delta T_{He} \cos(\omega t + \delta_2)$ in the temperature of the helium bath at frequency ω. Here δ_1 and δ_2 are arbitrary phase factors. A straightforward analysis using standard feedback theory shows that the change in the temperature of the bolometer is

$$\Delta T = \frac{(\varepsilon \Delta P_B / G)(1 + \omega^2 \tau_m^2)^{\frac{1}{2}} \cos(\omega t + \delta_1) + \Delta T_{He} \cos(\omega t + \delta_2)}{\tau \tau_m [(\omega^2 - \omega_o^2)^2 + \omega^2 / \tau_e^2]^{\frac{1}{2}}} . \qquad (3.1)$$

In Eq. (3.1), $\omega_o \approx (\alpha / \tau \tau_m)^{\frac{1}{2}} \sim 10$ Hz for typical values. Clearly, $\tau^{-1} > \omega_o > \tau_m^{-1}$. For a frequency $\omega << \tau_m^{-1}$, Eq. (3.1) simplifies to

$$\Delta T = [\varepsilon \Delta P_B / G\alpha] \cos(\omega t + \delta_1) + [\Delta T_{He} / \alpha] \cos(\omega t + \delta_2) \qquad (\omega << \tau_m^{-1}). \qquad (3.2)$$

We see that the feedback reduces the effect of either type of fluctuation by a factor $\alpha \simeq 50$. For a frequency $\omega >> \tau^{-1}$,

$$\Delta T = (\varepsilon \Delta P_B / G\omega\tau) \cos(\omega t + \delta_1) + (\Delta T_{He} / \omega^2 \tau \tau_m) \cos(\omega t + \delta_2) \qquad (\omega >> \tau^{-1}). \qquad (3.3)$$

In this limit, the change in the temperature of the bolometer is determined by the appropriate low pass thermal filters, and the feedback circuit plays no role.

/a calculation of the/

In Fig. 3 we plot/the relative squared response $(\Delta T)^2$ vs. frequency for fluctuations: (a) $(\Delta P_B)^2 \cos^2(\omega t + \delta_1)$ and (b) $(\Delta T_{He})^2 \cos^2(\omega t + \delta_2)$. The continuous line is the response without feedback, and the dashed line is the response in the presence of feedback. The following parameters were used: $\varepsilon = 1$, $C = 10^{-9} JK^{-1}$, $G = 5 \times 10^{-8} WK^{-1}$, $\tau_m = 20$ s, and $\alpha = 50$. At low frequencies, the effect of the perturbation on $(\Delta T)^2$ has been reduced by a factor of $\alpha^2 \approx 2{,}500$ by the feedback, whereas at high frequencies, the feedback has no effect.

3.3 Theoretical Noise Limits

A signal power $P_s \cos \omega t$ absorbed by, or generated on, the bolometer produces an rms voltage $V \cos\omega t$ across the bridge, where

$$V = \sqrt{2} I(\partial R/\partial T)\, P_s/G_e\, (1 + \omega^2\tau_e^2)^{-\frac{1}{2}} . \tag{3.4}$$

The correction ($\sim$ 10%) due to the attenuation of the signal by the bridge circuit has been neglected.

We now estimate the contributions of the various noise sources to the electrical NEP for typical values of the parameters, in order to determine which of the sources are most important. We consider only the case $\omega\tau << 1$, and assume throughout that $T = 1.2$ K, $G = 5 \times 10^{-8}$ WK^{-1}, $R = 1\,\Omega$, and $(\partial R/\partial T) = 10^3\ \Omega K^{-1}$. The thermal noise contribution is $(NEP)_{Th} = (4k_B T^2 G)^{\frac{1}{2}} \approx 2 \times 10^{-15}$ WHz$^{-\frac{1}{2}}$. The 1/f noise can be estimated from the work of Clarke and Hsiang[8] who measured the low-frequency noise in tin films at the superconducting transition. For films that were deposited on glass substrates, they found that the power spectrum of the noise voltage varied as 1/f, and was in good agreement with the prediction of Clarke and Voss[7]:

$$S_{1/f}(f) = \frac{J^2(\partial R/\partial T)^2\, k_B T^2}{C_F[3 + 2\, \ell n(\ell_1/\ell_2)]f} . \tag{3.5}$$

In Eq. (3.5), ℓ_1, ℓ_2, and C_F are the length, width, and heat capacity of the film, and J is the constant current bias. For the bolometer in a bridge circuit, Eqs. (3.4) and (3.5) lead to

$$(NEP)_{1/f} = G_e \{k_B T^2/C_F[3 + 2\, \ell n(\ell_1/\ell_2)]f\}^{\frac{1}{2}} . \tag{3.6}$$

$(NEP)_{1/f}$ is independent of I. If we take the film dimensions as $4 \times 0.25 \times 10^{-4}$ mm and use $C_F(Al) = 1.6 \times 10^{-4}$ JK^{-1} cm^{-3} at 1.2 K[19], we find that at 10 Hz $(NEP)_{1/f} \approx 10^{-14}$ WHz^{-1}. This estimate is a factor 5 higher than $(NEP)_{Th}$. However, Clarke and Hsiang[8] found that if the films were strongly thermally coupled to the substrate, the noise power spectrum flattened at low frequencies. The strong thermal coupling was achieved by depositing 5 nm of Al on the glass or sapphire substrate prior to the evaporation of the Sn. At 10 Hz, the power spectrum was reduced by a factor of 20 or more by this procedure. Thus, if a comparable flattening of the noise power spectrum occurs with Al films on sapphire, $(NEP)_{1/f}$ is expected to be comparable with $(NEP)_{Th}$. It is difficult to make *a priori* estimates of the low frequency noise in this regime, and one should not assume from the outset that this contribution is negligible.

The Johnson noise contribution is found by equating the rms signal voltage V from Eq. (3.4) with $(16k_BTR)^{\frac{1}{2}}$ (the extra factor of 2 arises from the demodulation scheme):

$$(NEP)_J = G_e(8k_BTR)^{\frac{1}{2}}/I(\partial R/\partial T) \quad . \tag{3.7}$$

$(NEP)_J$ decreases as I is increased. We can operate the bolometer at a current amplitude (say 2 μA) at which the Johnson noise is negligible compared with the thermal noise, and at which $I \ll [G/(\partial R/\partial T)]^{\frac{1}{2}}$. Thus, self-heating effects are negligible, and $G_e \approx G$.

Finally, we consider the contribution of the preamplifier noise. At frequencies above the 1/f noise region, the rms noise of our preampli-

fier with a source impedance of $10^5\ \Omega$ is about $2\ nVHz^{-\frac{1}{2}}$. This value corresponds to an rms voltage V_T of about $6 \times 10^{-12}\ VHz^{-\frac{1}{2}}$ referred to the input of the transformer (the cooled transformer does not contribute significantly to the preamplifier noise). Equating $\sqrt{2}\ V_T$ (the factor of $\sqrt{2}$ arises from the demodulation scheme) to V in Eq. (3.4), we find

$$(NEP)_A = V_T G_e / I(\partial R/\partial T) \ . \qquad (3.8)$$

Choosing I = 2 μA, we find $(NEP)_A \approx 2 \times 10^{-16}\ WHz^{-\frac{1}{2}}$, a value that is well below $(NEP)_{Th}$.

Provided that the 1/f noise in the Al film is reduced sufficiently by strong coupling of the film to the substrate, it is evident that the electrical NEP should be limited by the intrinsic thermal fluctuations of the bolometer for the values of the parameters we have chosen. It is, of course, necessary to make the contributions of the miscellaneous noise sources negligible. It seems impractical to make reliable *a priori* estimates of these contributions.

3.4 Experimental Measurements

The values of G, τ, and C were estimated with the feedback circuit disconnected and with $I << [G/(\partial R/\partial T)]$, so that $G_e \approx G$. First, we determined the resistance of the Al strip as a function of temperature. Second, the value of G was found by dissipating a known amount of power in the Bi heater and measuring the change in temperature. Third, an ac current of frequency (ω/2) was applied to the Bi heater, so that the bolometer temperature oscillated at frequency ω. By measuring the response of the bolometer as a function of frequency, we determined τ,

and hence $C = \tau G$. The responsivity was then determined with the bolometer in the feedback mode. A current at a low frequency $\omega/2$ was passed through the Bi heater, and the output of the closed loop was lock-in detected. From this measurement, we determined the responsivity of the bolometer referred to the output of the cooled transformer. The spectral density of the voltage noise at the output of the closed loop was measured using an on-line PDP-11[7] computer, and its value, referred to the output of the transformer, was calculated. From these two measurements the NEP was determined.

We evaluated the performance of five bolometers in some detail. Their important parameters are listed in Table I. The large range of values of dR/dT is evident. (Notice that the Al films on bolometers 1 and 2 did not have cut edges.) However, good values of the NEP could be obtained in each case by adjusting the bias current so that IdR/dT had the same value. Large bias currents are undesirable for low background operation because the high dissipation produced raises the temperature of the bolometer significantly above the bath temperature. Consequently, values of dR/dT below about 100 ΩK^{-1} were considered too low for practical bolometers. When the edges of the Al film were trimmed, values of dR/dT of 200 ΩK^{-1} or greater were always obtained. The bias current listed represent minimum values; higher values (up to a factor of 10 higher for the smaller bias currents) produced essentially the same value of NEP at frequencies near 5 Hz. This result indicates that the NEP was limited by thermal noise and/or 1/f noise in the film, rather than by Johnson noise or preamplifier noise.

The parameters for bolometer 5 are given in greater detail in Tables II and III. Table II lists the calculated heat capacities of the components of bolometer 5, and Table III lists its relevant measured electrical and thermal parameters. The measured heat capacity, 1.2×10^{-9} JK^{-1}, is in good agreement with the calculated value, 1.15×10^{-9} JK^{-1}. In Fig. 4 the dashed line represents the responsivity referred to the output of the bridge calculated from Eqs. (3.1) and (3.4) using the appropriate parameters from Table III. The roll-off below 1 Hz is due to the effect of the feedback system, and the roll-off above 1 Hz is due to the time constant of the bolometer. The dots are the measured responsivity, and are in excellent agreement with the calculated values. In Fig. 5, the dashed line is the sum of the thermal noise, Johnson noise, preamplifier noise, and bath noise power spectra referred to the bridge with the bolometer in the feedback mode. A power spectrum of 1.6×10^{-12} $(1\ Hz^2/f^2)\ K^2Hz^{-1}$ has been fitted to the data for the helium bath temperature fluctuations. Above 1 Hz, it is evident that the measured noise power spectrum is about a factor two greater than the calculated noise. It is likely that the excess noise arises from the intrinsic "1/f noise" of the Al film, which is expected to have a white power spectrum in this frequency range (see Section 3.3). The excess noise in the range 0.1 to 1 Hz probably arises from an instability in the feedback system. Fig. 6 shows the calculated and measured NEPs, obtained by taking the square root of the ratio of the data in Figs. 4 and 3. Above about 1 Hz, the measured NEP is somewhat higher than the calculated NEP. For example,

at 2 Hz the measured NEP is about 1.7×10^{-15} $WHz^{-\frac{1}{2}}$, compared with a thermal noise value of 1.3×10^{-15} $WHz^{-\frac{1}{2}}$. As the frequency increases, the NEP slowly degrades, for example, to 2.0×10^{-15} $WHz^{-\frac{1}{2}}$ at 5 Hz. This degradation reflects the fact that the responsivity falls as the frequency increases, while the Johnson noise and preamplifier noise remain constant. A slightly improved responsivity could probably have been obtained at the higher frequencies by operating the bolometer with a higher bias current. However, the thermal feedback would then be higher, and the bolometer nearer to thermal runaway.

The dynamic range of the bolometer is approximately $\delta T G/(NEP)$, where δT is the half-width of the transition and (NEP)/G is the temperature fluctuation per $Hz^{\frac{1}{2}}$. Taking $\delta T \sim 2$ mK and $(NEP)/G \sim 10^{-7}$ $KHz^{-\frac{1}{2}}$, we find a dynamic range of about 10^4 in a 1 Hz bandwidth. The maximum long-term change in temperature (due to a change in the background radiation or a change in the temperature of the helium bath) that can be cancelled by the feedback system is $\sim \alpha\delta T \sim 0.1$ K. This value corresponds to a change in background radiation of about 1 nW.

4. SNS BOLOMETER

4.1 Principle of Operation

A SNS Josephson junction consists of a layer of normal metal sandwiched between two superconductors.[10] Since the critical current of the junction rises rapidly as the temperature is lowered, the junction is a useful thermometer.

For metallurgical reasons, the preferred metals are lead for the superconductor and copper for the normal layer. We have found that the long term stability of SNS junctions is enhanced if the mean free path of the copper is shortened by alloying with a few percent of aluminum: this procedure minimizes the effect of lead diffusing into the copper. The copper is then in the dirty limit $\ell << \hbar v_F/2\pi k_B T$ (ℓ is the electronic mean free path, and v_F is the Fermi velocity). At low critical current densities, the supercurrent flows uniformly through the junction. For a square junction of side w, the critical current I_c is related to the critical current density I_o and to temperature by[10]

$$I_c = w^2 I_o = w^2 A \exp(- d/\xi_N) \quad . \tag{4.1}$$

Here, A is a temperature independent constant for temperatures below about $T_c/2$ (T_c is the transition temperature of the superconductor), and $\xi_N = (\hbar v_F \ell/6\pi k_B T)^{1/2}$ is the decay length of Cooper pairs in the normal metal[10]. When the critical current density becomes high enough, the current is excluded from the interior of the junction by its self field, and is confined to a peripheral strip whose width is of the order of the Josephson penetration depth

$$\lambda_J = [\hbar/2\ \mu_o(d + 2\lambda)e I_o]^{\frac{1}{2}} . \qquad (4.2)$$

In Eq. (4.2), λ is the penetration depth of the superconductor. Such a junction is said to be self-field limited (SFL). For a square junction of side w, self-field limiting becomes important when $\lambda_J \lesssim w/2$ (the exact numerical factor depends on the symmetry of the current feed[10]), or when the critical current $I_o w^2 \gtrsim 2\hbar/\mu_o(d + 2\lambda)e \sim 1$ mA for $(d + 2\lambda) \sim 0.5$ μm.

All of our more sensitive bolometers had critical currents considerably greater than 1 mA, and were heavily self-field limited. In this limit, the critical current is given by

$$I_c^{SFL} \propto I_o w \lambda_J = B \exp(-d/2\xi_N) = B \exp[-(T/T_o)^{\frac{1}{2}}] , \qquad (4.3)$$

where B is a temperature independent constant for $T \lesssim T_c/2$, and $T_o = 2\hbar v_F \ell/3\pi k_B d^2$. For $d \approx 0.5$ μm, $v_F \approx 10^6$ ms^{-1}, and $\ell \approx 10$ nm, we find $T_o \approx 0.06$ K.

The junction is biased with a constant current I greater than I_c, so that changes in critical current are measured as changes in the voltage across the junction. The voltage V across a heavily SFL junction is related to the junction resistance R (typically 2 μΩ), I, and I_c by the approximate expression

$$V = R(I - I_c) . \qquad (4.4)$$

From Eqs. (4.3) and (4.4) we can readily calculate

$$\left(\frac{\partial V}{\partial T}\right)_I^{SFL} = \frac{R I_c}{2(T T_o)^{\frac{1}{2}}} . \qquad (4.5)$$

Since $(\partial V/\partial T)_I$ is proportional to I_c, the advantage of using high critical currents (i.e. SFL junctions) is evident. For a SFL junction, with

$R = 2\ \mu\Omega$, $I_c = 50$ mA, $T = 2$ K, and $T_o = 0.06$ K, we find $(\partial V/\partial T)_I^{SFL} \approx 1.4 \times 10^{-7}\ VK^{-1}$.

The value of I/I_c is typically 1.01. For $I_c = 50$ mA and $R = 2\ \mu\Omega$, we find $V = 10^{-9}$ V, and the dissipated power is approximately 5×10^{-11} W. The thermal feedback is positive: an increase in temperature decreases I_c and thereby increases V. However, the thermal feedback is negligible; typically, $I(\partial V/\partial T)_I \approx 7 \times 10^{-9}\ WK^{-1}$, a value that is about 10 times smaller than G. The electrical responsivity for $\omega\tau << 1$ is given by Eq. (2.1), with $G \approx G_e$ and $\tau = \tau_e$, and Eq. (4.5):

$$S = RI_c/2(TT_o)^{\frac{1}{2}}\ G\ . \tag{4.6}$$

Using $RI_c/2(TT_o)^{\frac{1}{2}} \approx 1.4 \times 10^{-7}\ VK^{-1}$ and $G \approx 5 \times 10^{-8}\ WK^{-1}$, we find $S \approx 3\ VW^{-1}$.

4.2 Experimental Details

The bolometers were fabricated on $8 \times 4 \times 0.135$ mm single-crystal sapphire substrates (see Fig. 7). The sapphire substrate was mounted on nylon threads in the way described in Section 3.2, with a final coating of Pb to make the leads superconducting at 4.2 K. The junction was constructed as follows: first, a 10 nm film of Cu/Al (3% wt. Al) was deposited on the substrate to improve the adherence of the Pb films. Second, a strip of Pb $\sim$ 150 μm wide and $\sim$ 0.5 μm thick was evaporated. Third, a disk and a square sheet (the heater) of Cu/Al $\sim$ 0.4 μm thick were flash-evaporated from a series of pellets. Finally, a second strip of Pb was deposited to form the SNS junction.

The bolometer mount was attached to the top-plate of a vacuum can

(see Section 3.2), and superconducting leads (solder-coated copper) from the SNS junction and the heater were brought through the top of the can in a vacuum feedthrough. The leads from the junction were connected in series with a resistor, R_s, (1.1 μΩ) and the input coil of a S.H.E. corporation SQUID, as shown in Fig. 7. The SQUID was mounted in a solder-coated brass can just above the vacuum can, and the SQUID, vacuum can, series resistor, and connecting leads were enclosed in a can made of lead foil. Two concentric μ-metal cylinders around the cryostat reduced the ambient magnetic field to ∿ 1 μT. This precaution largely eliminated vibrational noise, and ensured that the critical current of the SNS junction was not significantly reduced. Pairs of current leads were attached to the SNS junction, the heater, and the series resistor (see Fig. 7). Current to the leads was provided by stabilized supplies that contributed a negligible level of noise. The rms current noise of the SQUID referred to the input coil was $4 \times 10^{-10}\,\mathrm{AHz}^{-\frac{1}{2}}$, an order of magnitude smaller than the Johnson noise current of the standard resistor and junction in series. The electrical time constant of the voltmeter was about 0.1 s.

Above the λ-point, the temperature of the helium bath was regulated with a manostat. Below the λ-point, regulation was provided by an electronic feedback circuit that employed a carbon resistance thermometer and a heater in the liquid helium.

4.3 Theoretical Noise Limits

We estimate the contributions of the various noise sources to determine which of the sources are dominant. We assume that $\omega\tau \ll 1$, $T \approx 2$ K, $G \approx G_e \approx 5 \times 10^{-8}$ WK^{-1}, and $S \approx 3$ VW^{-1}. The thermal fluctuation noise, $(NEP)_{Th}$, is 3.3×10^{-15} $WHz^{-\frac{1}{2}}$. The 1/f noise can be estimated from the work of Clarke and Hawkins[9] who studied the 1/f noise in shunted Josephson tunnel junctions, and concluded that an appropriately modified version of the thermal fluctuation theory of Clarke and Voss[7] was in excellent agreement with the measured noise. This theory predicts that the 1/f noise voltage has a spectral density

$$J_{1/f}(f) = \frac{(\partial V/\partial T)^2 I^2 k_B T^2}{3 C_J f} \cdot \tag{4.7}$$

In Eq. (4.7), $C_J = w^2[C_v(Cu)d + 2\, C_v(Pb)\xi]$, where $C_v(Cu)$ and $C_v(Pb)$ are the specific heats of Cu and Pb, and ξ is the Ginzburg-Landau coherence length. From Eqs. (4.5)-(4.7), we find

$$(NEP)_{1/f} = \frac{[J_{1/f}(f)]^{\frac{1}{2}}}{S} = G\left(\frac{k_B T^2}{3 C_J f}\right)^{\frac{1}{2}} \cdot \tag{4.8}$$

Inserting the values $w = 150$ μm, $d = 0.5$ μm, $\xi = 80$ nm, $C_v(Cu) = 2.5 \times 10^{-4}$ JK^{-1} cm^{-3}, and $C_v(Pb) = 1.0 \times 10^{-3}$ JK^{-1} cm^{-3}, we find $(NEP)_{1/f} \approx 2.7 \times 10^{-14}$ $WHz^{-\frac{1}{2}}$ at 10 Hz. This contribution is an order of magnitude higher than the estimated value of $(NEP)_{Th}$. However, as with the Al films, we expect that the low frequency noise will be appreciably lower if the films are strongly thermally coupled to the substrate[8]. Following the work of Clarke and Hsiang[8], one would expect the noise power spectrum to flatten at frequencies below $D/\pi L^2 \sim 10$ kHz, where $D \sim 10$ cm^2 sec^{-1} is the thermal diffusivity of the junction materials and $L \sim 150$ μm is

the width of the junction. In that case, the power spectrum at 10 Hz would be reduced by three orders of magnitude to a value roughly 50 times smaller than the Johnson noise spectral density. We, therefore, expect the "1/f" contribution to be negligible. However, it is evident that a proper measure of the low frequency fluctuations can be obtained only from experiment.

We next calculate the (modified) Johnson noise contribution of the junction, assuming that the result for a non-SFL shunted Josephson tunnel junction is applicable to the SFL case. The spectral density of the voltage fluctuations is[20]

$$J_J(f) = [1 + \tfrac{1}{2}(I_c/I)^2]4k_BTR \ . \qquad (4.9)$$

Using the values $(I_c/I) \approx 1$, T = 2 K, R = 2 μΩ, and S = 3 VW^{-1}, we find $(NEP)_J = [J_J(f)]^{\frac{1}{2}}/S \approx 6 \times 10^{-15}$ $WHz^{-\frac{1}{2}}$. This contribution is a factor of 2 higher than the thermal noise.

Finally, we consider the SQUID noise. For resistances of the order of 1 μΩ, the noise temperature of the SQUID voltmeter[11] is much less than 1 K. The voltmeter noise is thus quite negligible compared with the Johnson noise.

4.4 Experimental Results

The current-voltage (I-V) characteristics of the junction were obtained using the SQUID and standard resistor as a null-balancing voltmeter. The critical current increased rapidly with decreasing temperature as expected; the temperature dependence for a typical bolometer is shown in Fig. 8. The flattening of the curve at low temperatures is due to self-field limiting. For critical currents >> 1 mA, the I-V characteristics were well represented by Eq. (4.4).

The thermal conductance of the Pb-coated threads was measured by dissipating a known power in the heater and measuring the reduction in I_c. The measured temperature dependence of I_c was used to find the increase in temperature, ΔT, and the thermal conductance was calculated from $G = \Delta P/\Delta T$. The thermal conductance of the four leads of a typical bolometer is plotted vs. temperature in Fig. 9. The thermal conductance of the leads was apparently dominated by the lead, since the estimated conductance for the nylon threads is $\sim 4 \times 10^{-10} WK^{-1}$ at 1.5 K. The thermal conductance varies as $T^{4.4}$; for two other bolometers, the thermal conductance was found to vary as $T^{4.3}$ and $T^{4.9}$. This temperature dependence is not understood. The thermal conductance of the lead films well below T_c is dominated by phonons whose mean free path is boundary limited. The thermal conductance should therefore vary as the heat capacity, and exhibit a T^3 dependence[21].

The thermal time constant $\tau = C/G$ of the bolometer was measured by passing a steady current through the heater, with the SNS junction biased above I_c. The current was switched off, and the exponential decay of the SQUID output was measured with an oscilloscope or a chart recorder. The time

constant was a few tenths of a second between 2 K and 4.2 K. For an earlier version of the bolometer, in which the nylon threads were attached to the substrate with GE 7031 varnish, the time constant was several seconds: the heat capacity of the varnish was an order of magnitude higher than the heat capacity of the substrate and metal films.

We measured the responsivity of the bolometer by supplying a known power to the bolometer heater with the junction biased at 1.01 I_c and measuring the change in the output voltage of the flux-locked SQUID (which had a calibrated voltage amplification). Measured values of the responsivity are plotted vs. temperature in Fig. 10. The line represents the responsivity calculated from Eq. (4.6) with $\omega = 0$ and using measured values of R, I_c, T_o, and G. The agreement is good over most of the temperature range. The strong temperature dependence of the responsivity arises from the rapid increase of I_c and the rapid decrease of G as the temperature is lowered. At 1.3 K, the lowest temperature at which measurements were made, the measured responsivity was 2.9 VW^{-1}.

The noise in the bolometer was determined by measuring the rms voltage noise at the output of the flux-locked SQUID. The NEP, obtained by dividing the noise by the responsivity, is plotted in Fig. 11 as a function of temperature. The solid line represents the calculated NEP limited by the Johnson noise in the SNS junction and standard resistor, and the dashed line represents the NEP limited by thermal noise with $\omega\tau \ll 1$. It is evident that the NEP is limited by the Johnson noise. The best NEP obtained was $5 \times 10^{-15}\,WHz^{-\frac{1}{2}}$ at 1.73 K and 1.40 K; at the lower temperature, this value was a factor of 5 above the thermal noise. A more careful optimization of junction parameters (increasing I_c and de-

creasing T_o) should increase the responsivity sufficiently to make the Johnson noise contribution comparable to or less than the thermal fluctuation noise.

5. SIN BOLOMETER

Both superconductor-insulator-superconductor (SIS) and superconductor-insulator-normal metal (SIN) quasiparticle tunnel junctions are good candidates for thermometers on composite bolometers. Although we have not operated a bolometer of this type, for completeness, we briefly consider the performance of an SIN bolometer.

At temperatures well below T_c, the dynamic resistance of an SIN tunnel junction is equal to the normal state resistance, R_{NN}, for voltages well above Δ/e (Δ is the energy gap of the superconductor), but much higher than R_{NN} for voltages less than Δ/e. At voltages, V, below Δ/e, the dynamic resistance is strongly temperature dependent, and the junction is therefore useful as a thermometer. For $|V| < \Delta/e$, the quasiparticle current for a SIN junction is given by[12] the BCS theory:

$$I = \frac{2\Delta}{eR_{NN}} \sum_{m=1}^{\infty} (-1)^{m-1} K_1(m\Delta/k_BT) \sinh(meV/k_BT) \quad . \tag{5.1}$$

Here, K_1 is the modified Bessel function of the second kind. For $k_BT/\Delta << 1$ (i.e. $T << T_c$), Eq. (5.1) can be approximated as

$$I \approx \frac{(2\pi\Delta k_BT)^{\frac{1}{2}}}{eR_{NN}} \exp(-\Delta/k_BT)\sinh(eV/k_BT) \quad , \quad (\Delta/k_BT >> 1) \quad . \tag{5.2}$$

If we bias the junction with a fixed current and assume $eV \ll \Delta$, we find by differentiating Eq. (5.2) with respect to T:

$$\left(\frac{\partial V}{\partial T}\right)_I \approx \frac{V}{T} - \frac{\Delta}{eT}\left(1 + \frac{k_B T}{2\Delta}\right)\tanh\left(\frac{eV}{k_B T}\right) \approx \frac{V}{T}\left[1 - \frac{\Delta}{eV}\tanh\frac{eV}{k_B T}\right] \qquad \left(\frac{k_B T}{\Delta}, \frac{eV}{\Delta} \ll 1\right). \quad (5.3)$$

Differentiating Eq. (5.3) with respect to V, we find that $(\partial V/\partial T)_I$ is a maximum at $\cosh(eV/k_B T) \approx (\Delta/k_B T)^{\frac{1}{2}}$ or $V_{max} \approx (k_B T/e)\ln 2(\Delta/k_B T)^{\frac{1}{2}}$. The maximum value of $(\partial V/\partial T)_I$ is thus

$$\left(\frac{\partial V}{\partial T}\right)_I^{max} \approx \frac{k_B}{e}\ln 2(\Delta/k_B T)^{\frac{1}{2}} - \frac{\Delta}{eT}\tanh[\ln 2(\Delta/k_B T)^{\frac{1}{2}}] \approx -\Delta/eT \qquad \left(\frac{k_B T}{\Delta}, \frac{eV}{\Delta} \ll 1\right). \quad (5.4)$$

If the superconductor is Pb, $\Delta/e \approx 1.4$ mV, and at 1.5 K with $G \approx 5 \times 10^{-8}$ WK^{-1} and $\omega\tau \ll 1$, we find from Eq. (2.1) $S = |(\partial V/\partial T)^{max}|/G \approx 2 \times 10^4$ VW^{-1}.

To calculate the Johnson noise, we require the dynamic resistance, R_d. From Eq. (5.2), we find

$$R_d = \left(\frac{\partial V}{\partial I}\right)_T \approx R_{NN}\left(\frac{k_B T}{2\pi\Delta}\right)^{\frac{1}{2}} e^{\Delta/k_B T}\,\mathrm{sech}(eV/k_B T) \quad (\Delta/k_B T \gg 1). \quad (5.5)$$

At V_{max},

$$R_d(V_{max}) \approx \frac{R_{NN} k_B T e^{\Delta/k_B T}}{(2\pi)^{\frac{1}{2}}\Delta}. \quad (5.6)$$

An estimate of the Johnson noise limit on the NEP for $\omega\tau \ll 1$ is given by[22]

$$(NEP)_J \approx G[4k_B T R_d(V_{max})]^{\frac{1}{2}}/|(\partial V/\partial T)^{max}|$$

$$\approx 2^{3/4}\pi^{-\frac{1}{4}}\, e k_B T^2 G R_{NN}^{\frac{1}{2}} \exp(\Delta/2k_B T)\,\Delta^{-3/2}. \quad (5.7)$$

For a given superconductor, and for fixed G and T, we can evidently vary R_{NN} to change the NEP. With $G = 5 \times 10^{-8}$ WK^{-1}, $T = 1.5$ K, $\Delta/e = 1.4$ mV, $(NEP)_J$ is made equal to $(NEP)_{Th} = 2.5 \times 10^{-15} WHz^{-\frac{1}{2}}$ with $R_{NN} \approx 0.02$ Ω. The corresponding value of $R_d(V_{max})$ is about 32 Ω. Thus, the dynamic resistance can be matched optimally to the preamplifier by a cooled transformer.

It appears to be difficult to fabricate high quality SIN tunnel junctions with R_{NN} as low as 0.02 Ω. Preliminary experiments indicated that Ni-NiOx-Pb/In junctions were relatively stable with respect to storage and thermal cycling, but contained resistive shorts that lowered both $(\partial V/\partial T)_{max}$ and $R_d(V_{max})$ below the ideal values. For a typical junction at 1.3 K, $(\partial V/\partial T) \approx 3 \times 10^{-4}$ VK^{-1} and $R_d \approx 10$ Ω at a bias current of 15 μA. Although this junction was not operated as a bolometer, its responsivity with $G \approx 5 \times 10^{-8}$ WK^{-1} would have been about 6×10^3 VW^{-1}, and its Johnson noise limited NEP at 1.3 K would have been about 5×10^{-15} $WHz^{-\frac{1}{2}}$. This performance is not as good as the ideal value derived above, but indicates that a junction of somewhat higher quality could approach the sensitivity of the transition edge thermometer. It would have the advantage of a broader range of operating temperature.

6. FAR INFRARED ABSORBER

6.1 Theory

The portions of the bolometer that can absorb a significant amount of infrared radiation are the dielectric substrate and the conducting film. Both sapphire and (most types of) diamond have absorption bands in the near infrared. At far infrared wavelengths where these composite structures are expected to be most useful, however, the cold substrate acts as an essentially lossless dielectric with an index of refraction which is only weakly dependent on frequency. The substrate serves to impedance match free space radiation into a thin metal film deposited on the back side of the bolometer. The surface impedance of the film is selected for optimum absorption. We calculate the absorptivity under the following assumptions: The absorbing layers comprise an infinite plane; the sapphire has a thickness d, a refractive index n (we neglect birefringence), and a permeability equal to that of free space; the conducting layer has an infrared frequency resistivity per square, $R_{\square}$, that is the same as at zero frequency, and a thickness that is much smaller than the skin depth and the wavelength of the radiation; the radiation is unpolarized; the radiation makes only a single pass at the bolometer (i.e. there is no reflecting surface under the bolometer); and the radiation is incident normally on the surfaces.

The transmission and reflection coefficients at the upper (uncoated surface) are[23]

$$T_1 = 4n/(n + 1)^2 , \tag{6.1}$$

and

$$R_1 = (n - 1)^2/(n + 1)^2 . \tag{6.2}$$

The transmission, reflection, and absorption coefficients at the lower (coated) surface are

$$T_2 = 4n/(n + 1 + Z_o/R_\square)^2 \ , \tag{6.3}$$

$$R_2 = (1 - n + Z_o/R_\square)^2/(n + 1 + Z_o/R_\square)^2 \ , \tag{6.4}$$

and $$A_2 = (4nZ_o/R_\square)/(n + 1 + Z_o/R_\square)^2 \ , \tag{6.5}$$

where Z_o ($\approx 377\ \Omega/\square$) is the impedance of free space. Although Eqs. (6.1) to (6.5) are derived for normal incidence, they remain accurate to within a few percent for angles of incidence up to 60°. In general, there will be multiple reflections between the two surfaces of the substrate, giving rise to Fabry-Pérot fringes in the observed values of the transmissivity, T_b, reflectivity, R_b, and absorptivity, A_b, of the bolometer. It can readily be shown that

$$T_b = \frac{T_1 T_S T_2}{1 + T_S^2 R_1 R_2 \pm 2T_S \sqrt{R_1 R_2}\cos\delta} \ , \tag{6.6}$$

$$R_b = \frac{R_1 + T_S^2 R_2 - 2T_S \sqrt{R_1 R_2}\cos\delta}{1 + T_S^2 R_1 R_2 \pm 2T_S \sqrt{R_1 R_2}\cos\delta} \ , \tag{6.7}$$

and $$A_b = \frac{T_1(1 - T_S T_2 - T_S^2 R_2)}{1 + T_S^2 R_1 R_2 \pm 2T_S \sqrt{R_1 R_2}\cos\delta} \ . \tag{6.8}$$

The plus sign applies when $Z_o/R_\square > n - 1$, and the minus sign applies when $Z_o/R_\square < n - 1$. In these equations, T_S is the transmissivity of a thickness d of sapphire, $\delta = 4\pi nd\bar{\nu}$, and $\bar{\nu}$ is the free-space wavenumber of the radiation. In practice, all three expression will be complicated by the fact that sapphire is birefringent.

A particular simple case arises when the reflection from the metal film $R_2 = 0$, that is when $Z_o/R_\square = n - 1$ [from Eq. (6.4)]. There are no multiple reflections within the sapphire, and the absorptivity of the bolometer is independent of frequency. With $T_S = 1$, we find

$$A_b(Z_o/R_\square = n - 1) = 4(n - 1)/(n + 1)^2 \ . \qquad (6.9)$$

If we take $n \approx 3$, as is appropriate for sapphire, we find $A_b(Z_o/R_\square = n - 1) \approx 0.5$. Any other value of n produces a smaller value of the frequency-independent absorptivity. If the bolometer is to be used over a wide range of frequencies, it is usually desirable to choose $R_\square = Z_o/(n - 1) \approx Z_o/2$, so that the absorption is frequency-independent. On the other hand, if the bolometer is to be used over a relatively narrow frequency band, one can take advantage of the Fabry-Pérot fringes to obtain a higher absorptivity. As an example, take $\delta = 2\pi$, corresponding to the case $\bar{\nu} = 1/2nd$, and $T_S = 1$. If $d = 0.05$ mm, and $n = 3$, the absorptivity has a peak at about 33 cm^{-1}, and has minima at about 17 cm^{-1} and 50 cm^{-1}. The peak absorptivity is found by setting $\cos \delta = 1$ in Eq. (6.8), and maximizing A_b with respect to $Z_o/R_\square$ (with $T_S = 1$). If we assume $n = 3$, we find that the maximum value of A_b is 0.90, with $Z_o/R_\square = 10$. In practice, the Fabry-Pérot pattern for sapphire will be complicated by the presence of the extraordinary ray (for which $n \approx 3.3$), and will depend on the cut of the sapphire crystal. No such complications arise for diamond, which is optically isotropic.

6.2 Experimental Characterization of Coated Substrates

Bismuth films varying in thickness from 30 nm to 480 nm were deposited on 8 × 4 × 0.135 mm sapphire substrates. Bismuth was used for the absorbing film because the required resistivity range could be achieved with a convenient range of thicknesses. Other materials, for example, chromium, /or nickel-chromium alloys/ would presumably work equally well. These substrates are optically polished on one side and are rough on the reverse side. The rough side has irregularities large compared with the thickness of the films, but small compared with far infrared wavelengths. For each film thickness, a sample was prepared on both smooth and rough surfaces. The resistivities of these films measured at 300 K and 4.2 K are shown in Fig. 12. The resistivities at 300 K are greater than the bulk value, and increase as the films are cooled to 4.2 K. These results suggest that the structure of the films is somewhat non-crystalline. Nevertheless, the resistivities were quite reproducible, and the desired resistance could be obtained readily.

The far infrared transmission of the coated substrates was measured at 1.3 K using a Fourier-transform spectrometer and a germanium bolometer. Transmissivity spectra were obtained for an empty sample holder, for an uncoated substrate, and for four substrates with varying film thicknesses. Measurements were made over three overlapping spectral ranges, from 3 to 25, 10 to 120, and 15 to 300 cm^{-1} with resolutions of 0.25, 1.2, and 3.0 cm^{-1}, respectively. Transmissivity spectra were obtained by dividing the transmission spectrum of each sample by the transmission spectrum of the empty sample holder. A series of transmissivity spectra is shown in Fig. 13. The Fabry-Pérot fringes are very pronounced for the uncoated

substrate, and have a period of about 12 cm^{-1} as expected for d = 0.135 mm and n ≈ 3. The beat pattern is due to the difference (∿ 0.3) in the refractive indices for the ordinary and extraordinary rays. The coated substrates show reductions in the overall transmission and in the amplitude of the Fabry-Pérot fringes. The latter effect is due to the reduced reflection at the back surface when it is coated with a conducting layer. According to Eq. (6.4), the reflectivity goes to zero (and hence the fringes vanish) when $R_{\square} = Z_o/(n - 1)$ ($\approx Z_o/2 \approx 188$ Ω/□ for sapphire). In Fig. 13, the minimum in the fringe amplitude occurs between $R_{\square} = 149$ and 235 Ω/□.

The Fabry-Pérot fringes enable us to determine R_b and A_b from measurements of T_b. Since the spectra do not change greatly over the frequency range 3 to 300 cm^{-1}, we obtained values of T_b, R_b, and A_b near the maximum in the beat pattern that occurs around 100 cm^{-1}. A complete analysis of the data is extremely complicated, and unwarranted in the present circumstances. We shall regard the sapphire transmissivity, T_S, as an empirical parameter that accounts for the frequency and polarization dependence of the refractive index, the surface roughness, and the angular divergence of the f/1.5 beam. First, the transmission and reflection coefficients at the uncoated surfaces and the value of T_S were determined by obtaining values of T_b from the measured maximum and minimum values near 100 cm^{-1} for the uncoated substrate and inserting them into Eq. (6.6) with $\cos\delta = +1$ and -1 respectively. We found $T_1 = 0.76$, $R_1 = 0.24$, and $T_S = 0.88$. Within experimental error, these values of T_1 and R_1 are consistent with $n = 3.0$[24]. The value of T_S is too small to represent a simple absorption in the sapphire, and arises

from the simplifications mentioned above.

The values of T_1, R_1, and T_S were used in Eq. (6.6) to obtain T_2 and R_2 for various film resistivities; T_2 and R_2 were used in Eqs. (6.7) and (6.8) to obtain R_b and A_b. Figure 14 shows the experimental values of the maxima and minima in T_b, R_b, and A_b as a function of $Z_o/R_\square$. There is no significant difference between the values measured with the bismuth on the rough and smooth surfaces. The lines are calculated from Eqs. (6.6) to (6.8) using the measured values of R_1, T_1, and T_S, and the values of R_2 and T_2 obtained from Eqs. (6.3) to (6.5) with the experimentally determined value of n. Considering the simplifications made in the theory, the general agreement between theory and experiment is reasonably good. In particular, an absorptivity of approximately 0.5 is obtained at $Z_o/R_\square \approx 2$, where the fringes have a small amplitude. For $Z_o/R_\square \approx 8$, the measured maximum absorptivity is approximately 0.8.

6.3 Far Infrared Efficiency of Bolometer

The far infrared absorptivity of the bolometer was measured by chopping the radiation falling on the top of the light pipe between sources at 77 K and 290 K. The transmissivity of the light pipe and of the various elements in the light pipe were measured separately, so that the power incident on the bolometer could be computed. The ratio of the absorbed power to the incident power was the absorptivity.

The cold source was contained in a 150 mm diameter glass dewar filled with liquid nitrogen. The lower part of the inside of the dewar was covered with AN-72 Eccosorb^{TM}, and the upper part was

covered with aluminum sheet which was in contact with the liquid nitrogen. The cold radiation traveling upward from the dewar was deflected downward into the light pipe by two polished aluminum mirrors. A circular aperture 29 mm in diameter limited the solid angle viewed by the light pipe. The separation between the aperture and the light pipe could be varied to change this solid angle. An 11 Hz reflecting chopper with its blades at 45° to the horizontal was located below the aperture so that the signal reaching the light pipe arrived alternately from the aperture and from an ambient temperature slate blackboard. The slate was a convenient reference because of its high absorptivity and long thermal time constant. The calibration was accomplished by measuring the difference between the lock-in detected signal from the cold source with the aperture open and the signal measured when an ambient temperature (290 K) piece of Eccosorb was place on top of the horizontal metal plate which contained the aperture.

The stainless steel light pipe (760 mm long and 11.7 mm i.d.) was sealed at the top with a 0.2 mm thick black polyethylene sheet. The vacuum can at the bottom was sealed with a wedge-shaped sapphire window that tapered in thicknes from 1.52 mm to 1.02 mm. A 2.54 mm thick Fluorogold^{TM} low-pass filter was placed in the liquid helium above the sapphire window to define the spectral bandpass and to reduce the background loading on the bolometer. The lower side of the bolometer substrate (4 × 4 × 0.05 mm) was coated with a 80 nm bismuth film with a resistance of approximately 190 Ω/□ at 1.5 K. Thus, the absorption was approximately independent of frequency. A slab of Eccosorb^{TM} was placed behind the bolometer to absorb the radiation which by-passed the bolometer

or was transmitted through it. Consequently, the radiation made only a single pass at the bolometer.

The transmissivity of the Fluorogold™ filter at 1.5 K was measured using a Fourier transform spectrometer, and is plotted in Fig. 15(a). Figure 15(b) shows the calculated difference between the blackbody sources at 290 K and 77 K as viewed through the Fluorogold™ filter. This curve represents the $\sim$ 5 to 45 cm^{-1} pass-band of the calibration. We estimate an error of ± 3% in the power calibration. The transmissivity of the light pipe measured at room temperature over the same range of frequencies and solid angles in a separate experiment was 0.61 ± 0.03. When the light pipe was cooled to liquid nitrogen temperatures, the transmissivity was unchanged within ± 2%. This value for T_{lp} can be brought into agreement with the calculated transmissivity from a light pipe theory which ignores paraxial rays[25], if we assume a resistivity which is three times larger than the measured low temperature value of approximately 70 μΩcm. Other experimentors have found a similar discrepancy.[25]

The transmissivity of the sapphire window at 1.5 K was measured to be 0.57 ± 0.02. This value is in excellent agreement with the calculated value of 0.57 obtained assuming refractive indices of 3.0 and 3.4 and assuming negligible absorption. The transmissivity of the black polyethylene window at room temperature was measured to be 0.86 ± 0.02. The absorbing area of the bolometer was reduced from 16 mm^2 to A_{eff} = 14.6 mm^2 by the superconducting In and Al films, which have negligible absorption in the far infrared. We assume that the fraction of the radiation leaving the light pipe which is incident

on the detector is equal to the ratio of A_{eff} to the area of the light pipe.

The far infrared responsivity of the bolometer was measured over a range of solid angles from 2.0 to 6.9×10^{-3} sr. As expected, the data show no significant dependence on solid angle. The average value of the absorptivity is 0.52 ± 0.05. The aggregate error limit of ± 0.05 is obtained by combining errors of $\pm 5\%$ in the measurements of the electrical NEP and the far infrared responsivity with values given above for the errors in the measurements of the transmissivity of the black polyethylene, the light pipe, the Fluorogold™, and the sapphire. This value is in excellent agreement with the theoretical value of 0.5 and the value of 0.5 obtained from the transmissivity measurements.

The effective absorptivity, $\&_e$ (relative to the area of the entire bolometer), is 0.47 ± 0.05. Using our best value of electrical NEP, $(1.7 \pm 0.1) \times 10^{-15} \mathrm{WHz}^{-\frac{1}{2}}$, we find $D^* = \&_e A^{\frac{1}{2}}/\mathrm{NEP} = (1.1 \pm 0.1) \times 10^{14}$ cm W^{-1} $\mathrm{Hz}^{\frac{1}{2}}$.

7. POSSIBLE IMPROVEMENTS

Of the three superconductive bolometers described, the transition edge bolometer is the most highly developed, and the simplest to fabricate and operate. There seems to be little advantage in going to the SNS or SIN versions unless a wider operating temperature range is desirable. Some improvements in the sensitivity of the transition edge bolometer appear possible. A diamond substrate would have a heat capacity of approximately $10^{-10}\,JK^{-1}$, a factor of six lower than the sapphire substrate. The bismuth heater could be eliminated, the number of indium contacts could be reduced to two, with somewhat smaller areas, and the bismuth absorber could be replaced by a much thinner chromium film. By means of these modifications, we estimate that the total heat capacity could be reduced by a factor of six to about $2 \times 10^{-10}\,JK^{-1}$. For the same value of thermal conductance, the time constant of the bolometer would be reduced to about 10 ms. Alternatively, the thermal conductance could be reduced to about $3 \times 10^{-9}\ WK^{-1}$, keeping the time constant at its present value, 60 ms. Provided that the bolometer was still essentially thermal noise limited, an improvement in the NEP by a factor of $\sqrt{6}$ could be expected.

A further improvement in sensitivity could be obtained by cooling the bolometer to liquid He^3 temperatures, and operating at about 0.4 K using a titanium film as the thermometer. We estimate that a bolometer using a sapphire substrate with the same dimensions as the present bolometer would have a heat capacity of $10^{-10}\,JK^{-1}$ or less, so that the thermal conductance could be reduced to $2 \times 10^{-9}\ WK^{-1}$ for a time constant

of about 50 ms. The thermal noise limited NEP ($\propto TG^{\frac{1}{2}}$) would then approach $10^{-16}\,WHz^{-\frac{1}{2}}$. In order to achieve this limit, a preamplifier with a noise temperature of less than 0.4 K would be required. The use of a diamond substrate would be expected to give a further improvement.

Acknowledgement

We wish to thank Dr. C. D. Andriesse for his careful reading of the manuscript.

References

†Work supported by U.S.E.R.D.A.

1. F. J. Low, J. Opt. Soc. Am. 51, 1300 (1961).

2. N. Coron, G. Dambier, and J. Leblanc, "Infrared Detection for Space Research", V. Manno and J. Ring, Eds. (D. Reidel, Dordrecht-Holland, 1971), pp. 121-131.

3. F. J. Low (private communication).

4. M. W. Werner, J. H. Elias, D. Y. Gezari, M. G. Hauser, and W. E. Westbrook, Astrophys. J. 199, L185 (1975).

5. N. S. Nishioka, P. L. Richards, and D. P. Woody (to be published).

6. D. H. Andrews, W. F. Brucksch, Jr., W. T. Ziegler, and E. R. Blanchard, Rev. Sci. Instrum. 13, 281 (1942); D. H. Martin and D. Bloor, Cryogenics 1, 159 (1961); D. Bloor, T. J. Dean, G. O. Jones, D. H. Martin, P. A. Mawer, and C. H. Perry, Proc. Roy. Soc. A260, 510 (1961); C. L. Bertin and K. Rose, J. Appl. Phys. 39, 2561 (1968); M. K. Maul, M. W. P. Standberg, and R. L. Kyhl, Phys. Rev. 182, 522 (1969); M. K. Maul and M. W. P. Standberg, J. Appl. Phys. 40, 2822 (1969); I. A. Khrebtov, N. M. Gropshtein, and G. A. Zaitsev, Prib. i Tek. Eksp. 1, 247 (1971); C. L. Bertin and K. Rose, J. Appl. Phys. 42, 163 (1971); R. M. Katz and K. Rose, Proc. IEEE 61, 55 (1973); N. A. Pankratov, G. A. Zaitsev, and I. A. Khrebtov, Cryogenics 13, 497 (1973); G. Gallinaro and R. Varone, Cryogenics 15, 292 (1975).

7. R. F. Voss and J. Clarke, Phys. Rev. B13, 556 (1976).

8. J. Clarke and T.-Y. Hsiang, Phys. Rev. B13, 4790 (1976).

9. J. Clarke and G. A. Hawkins, Phys. Rev. B14, 2826 (1976).

10. P. G. de Gennes, Rev. Mod. Phys. 36, 225 (1964); J. Clarke, Proc. Roy. Soc. A308, 447 (1969).

11. For a review, see, for example, J. Clarke, Proc. IEEE 61, 8 (1973).

12. For a review, see, for example, D. H. Douglas and L. M. Falicov, Prog. Low Temp. Phys., edited by C. J. Gorter (North-Holland, Amsterdam, 1964), Vol. 4, p. 97.

13. J. Clarke, G. I. Hoffer, and P. L. Richards, Rev. Phys. Appl. 9, 69 (1974).

14. J. Clarke, G. I. Hoffer, P. L. Richards, and N.-H. Yeh, Low Temperature Physics - LT14, M. Krusius and M. Vuorio, Eds. (American Elsevier, New York, 1975), Vol. 4, pp. 226-229; J. Clarke, P. L. Richards, and N.-H. Yeh, Appl. Phys. Lett. (submitted).

15. R. A. Smith, F. E. Jones, and R. P. Chasmar, The Detection and Measurements of Infra-Red Radiation (Oxford University Press, Oxford, 1968), 2nd ed.

16. See, for example, F. N. H. Robinson, Noise and Fluctuations in Electronic Devices and Circuits (Clarendon Press, Oxford, 1974).

17. M. Strongin, O. F. Kammerer, and A. Paskin, Phys. Rev. Lett. 14, 949 (1965).

18. D. E. Prober, Rev. Sci. Instrum. 45, 848 (1974).

19. Properties of Materials at Low Temperature, edited by V. J. Johnson (Pergamon, New York, 1961).

20. K. K. Likharev and V. K. Semenov, J.E.T.P. Lett. 15, 442 (1972).

21. C. Kittel, Introduction to Solid State Physics, 5th edition (John Wiley and Sons, New York, 1968).

22. This result is not actually the optimized NEP which would be obtained by minimizing $(4k_B TR_d)^{\frac{1}{2}}/(\partial V/\partial T)$. However, Eq. (5.7) enables us to estimate a typical NEP.

23. M. Born and E. Wolf, Principles of Optics (Pergamon Press, Oxford, 1975), 5th edition, pp. 628-632.

24. E. V. Loewenstein, D. R. Smith, and R. L. Morgan, Appl. Optics 12, 398 (1973).

25. R. C. Ohlmann, P. L. Richards, and M. Tinkham, J. Opt. Soc. Am. 48, 531 (1958).

Table I. Parameters of five transition edge bolometers

Bolometer	1	2	3	4	5
Dimensions (mm)	2×4×0.135	2×4×0.135	2×4×0.135	2×4×0.135	4×4×0.050
T (K)	1.30	1.28	1.40	1.28	1.27
dR/dT (ΩK^{-1})	60*	80*	2,000	800	200
G ($10^{-8} WK^{-1}$)	2.5	4	3.5	3.5	2
τ (s)	0.1	0.05	0.05	0.05	0.08
I (μA rms)	14	11	0.7	0.7	5
NEP (5 Hz) ($10^{-15} WHz^{-\frac{1}{2}}$)	5	3	3	3	2

*Al films did not have cut edges.

Table II. Calculated heat capacities at 1.27 K of components of bolometer 5

Component	Dimensions (mm)	Heat capacity (10^{-10} JK^{-1})
Sapphire	4 × 4 × 0.050	6.6
In films (4)	0.5 × 0.175 × 0.0029	2.8
Bi heater	4 × 0.5 × 0.000088	0.2
Al thermometer	4 × 0.18 × 0.000070	0.1
Bi absorber	4 × 4 × 0.000093	1.8
		11.5

Table III. Measured parameters of bolometer 5

Operating temperature	1.27 K
G	2.0×10^{-8} WK^{-1}
τ	60 ms
C	1.2×10^{-9} JK^{-1}
dR/dT	200 ΩK^{-1}
I	5.3 μA rms
G_e	1.44×10^{-8} WK^{-1}
τ_e	83 ms
$S = (\partial V/\partial T)/G_e$ (2 Hz)	8.6×10^{4} VW^{-1}
τ_m	25 s
α	70
NEP measured	$(1.7 \pm 0.1) \times 10^{-15}$ $WHz^{-\frac{1}{2}}$ at 2 Hz
$(NEP)_{Th}$	1.3×10^{-15} $WHz^{-\frac{1}{2}}$
Dynamic range in 1 Hz bandwidth	10^4
Power spectrum of bath fluctuations	1.6×10^{-12} $(1\ Hz^2/f^2)$ K^2Hz^{-1}
Effective absorptivity, ε_e	0.47 ± 0.05
D*	$(1.1 \pm 0.1) \times 10^{14}$ cm W^{-1} $Hz^{\frac{1}{2}}$

Figure Captions

1. Configuration of superconducting transition edge bolometer and mount.
2. Schematic of electronics for superconducting transition edge bolometer.
3. Calculated relative response $(\Delta T)^2$ of bolometer vs. frequency for perturbations: (a) $(\Delta P_B)^2 \cos^2(\omega t + \delta_1)$ and (b) $(\Delta T_{He})^2 \cos^2(\omega t + \delta_2)$, with (---) and without (——) feedback.
4. Measured (•) and calculated (---) responsivity of transition edge bolometer (referred to output of bridge).
5. Measured (•) and calculated (---) noise power spectrum of transition edge bolometer (referred to output of bridge).
6. Measured (•) and calculated (---) NEP of transition edge bolometer.
7. SNS bolometer and electronics.
8. Critical current vs. temperature for typical SNS bolometer.
9. Thermal conductance of the four leads (each approximately 5 mm long) vs. temperature for typical SNS bolometer.
10. Responsivity vs. temperature for typical SNS bolometer. Dots are measured responsivity, and the line is calculated from other measured parameters.
11. NEP vs. temperature for typical SNS bolometer. Dots are measured values, continuous line is calculated Johnson noise-limited NEP, and dashed line is calculated thermal noise limited NEP.
12. Measured dc resistivity of bismuth films on rough and smooth sapphire surfaces vs. film thickness.
13. Transmissivity spectra for sapphire substrates coated with bismuth films of various resistances.

14. Maximum and minimum values of the Fabry-Pérot fringes in the transmissivity (a), reflectivity (b), and absorptivity (c) as a function of the resistance of the bismuth film. Dots and squares are experimental values near 100 cm^{-1} with the bismuth on the smooth and rough sides of the sapphire respectively, while the lines represent the calculated values.

15. (a) Measured transmissivity of 2.54 mm thick Fluorogold™ filter at 1.5 K. (b) Normalized intensity distribution of difference between the blackbody sources at 290 K and 77 K viewed through the filter in (a).

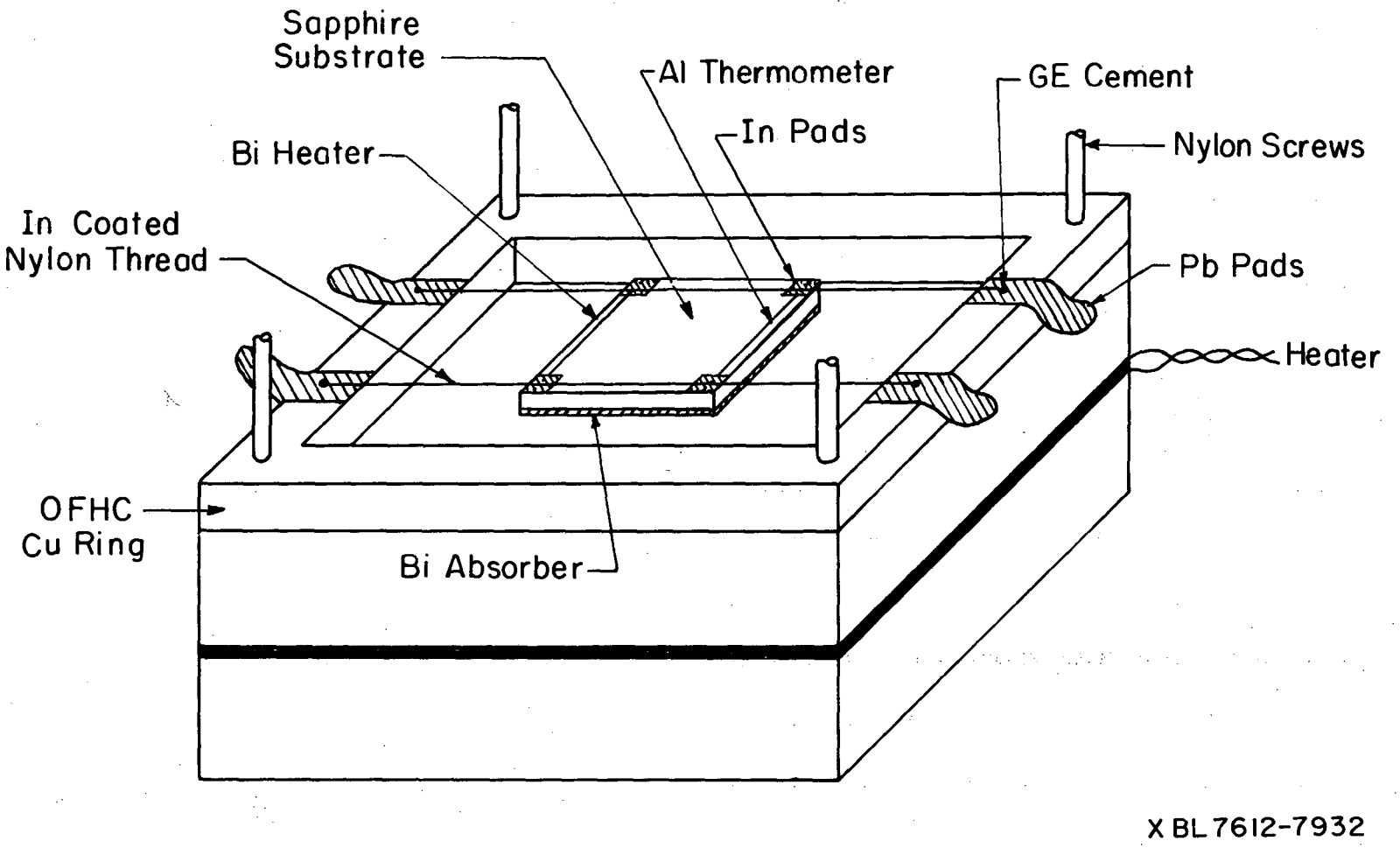
Sapphire
Substrate
Al Thermometer
GE Cement
In Pads
Bi Heater
Nylon Screws
In Coated
Nylon Thread
Pb Pads
Heater
OFHC
Cu Ring
Bi Absorber
XBL7612-7932

Fig. 1

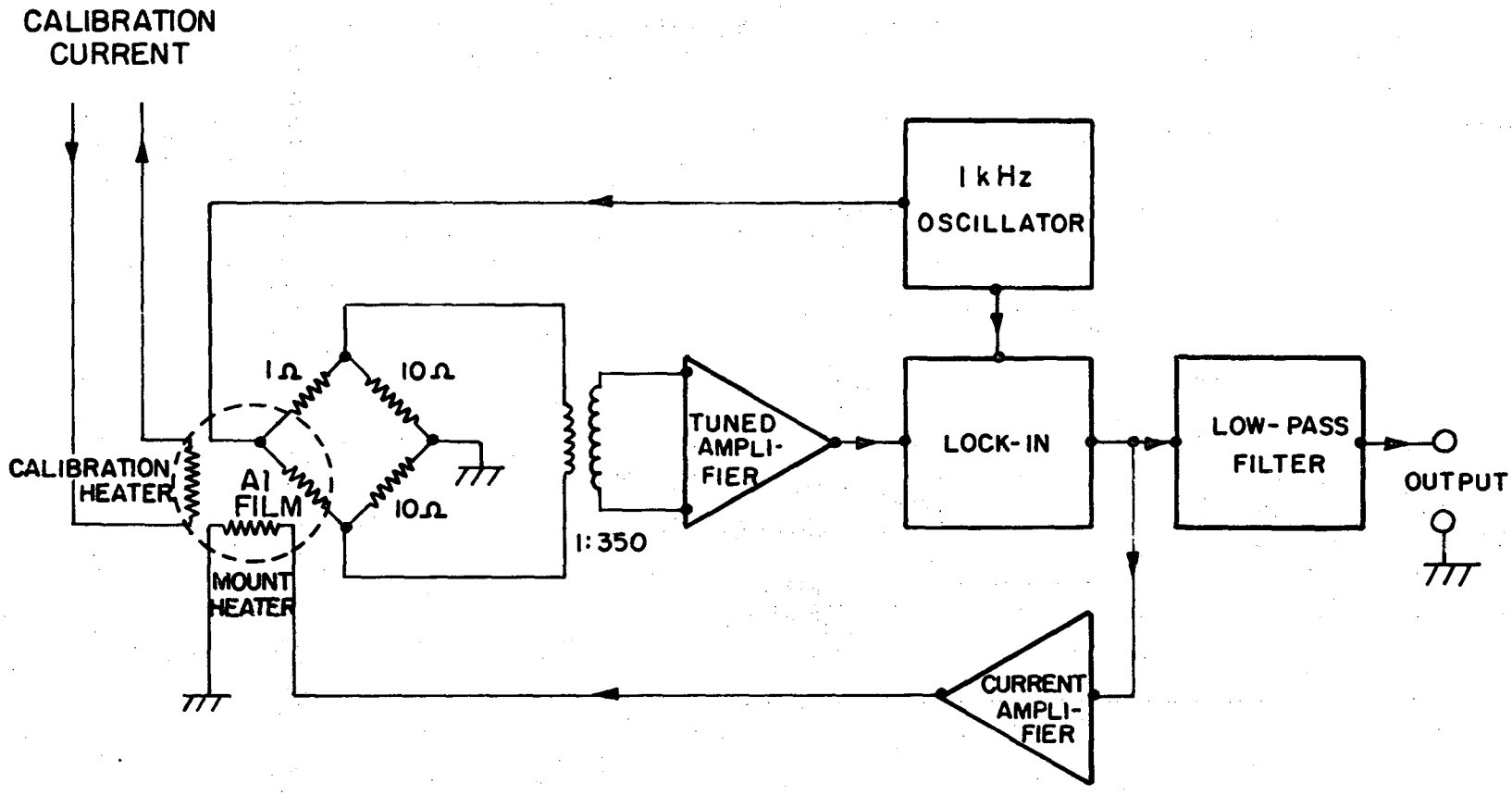

XBL 771-4928

Fig. 2

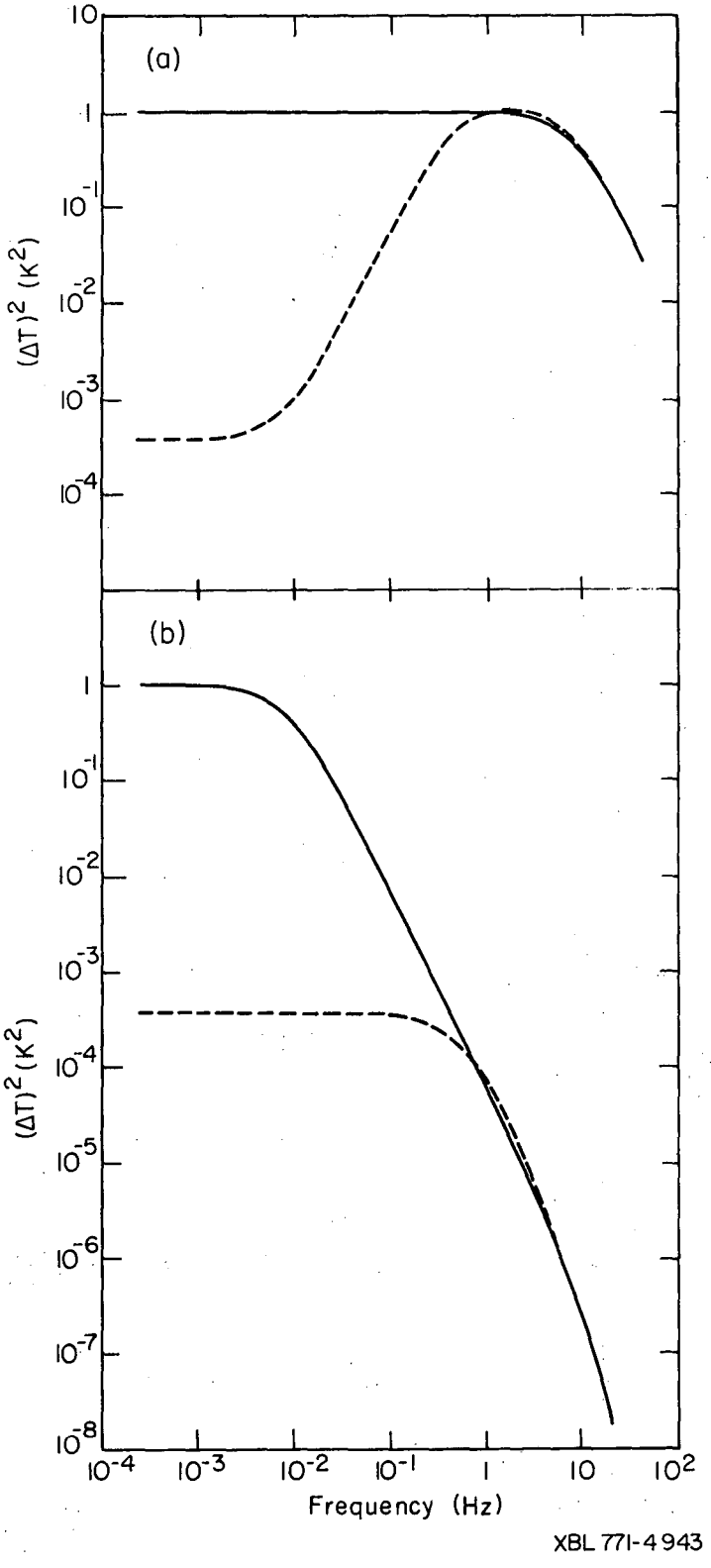
(a)
(b)
$(\Delta T)^2$ (K^2)
$(\Delta T)^2$ (K^2)
10
1
10^{-1}
10^{-2}
10^{-3}
10^{-4}
10^{-5}
10^{-6}
10^{-7}
10^{-8}
10^{-4}
10^{-3}
10^{-2}
10^{-1}
1
10
10^{2}
Frequency (Hz)
XBL 771-4943

Fig. 3

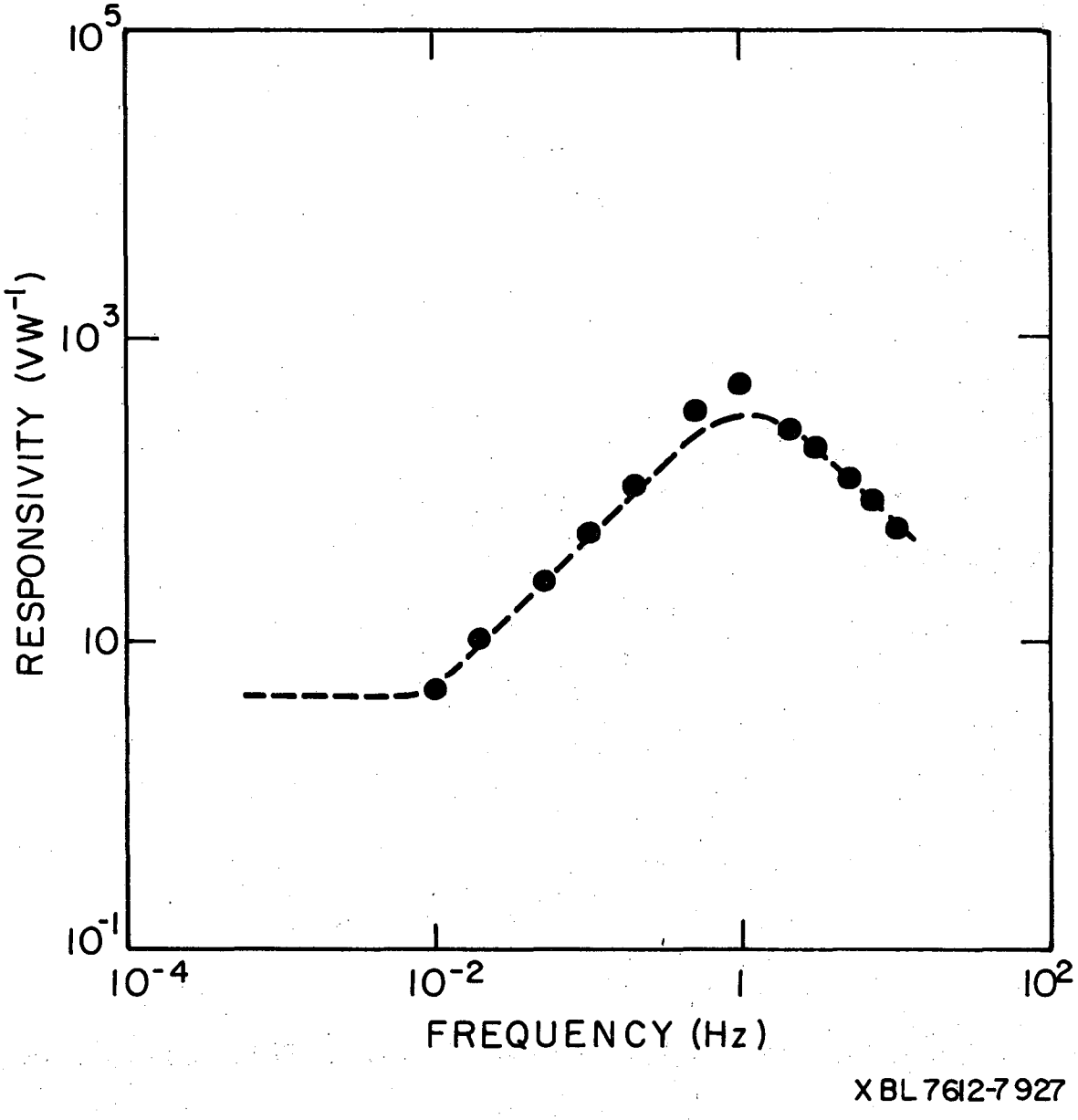

Fig. 4

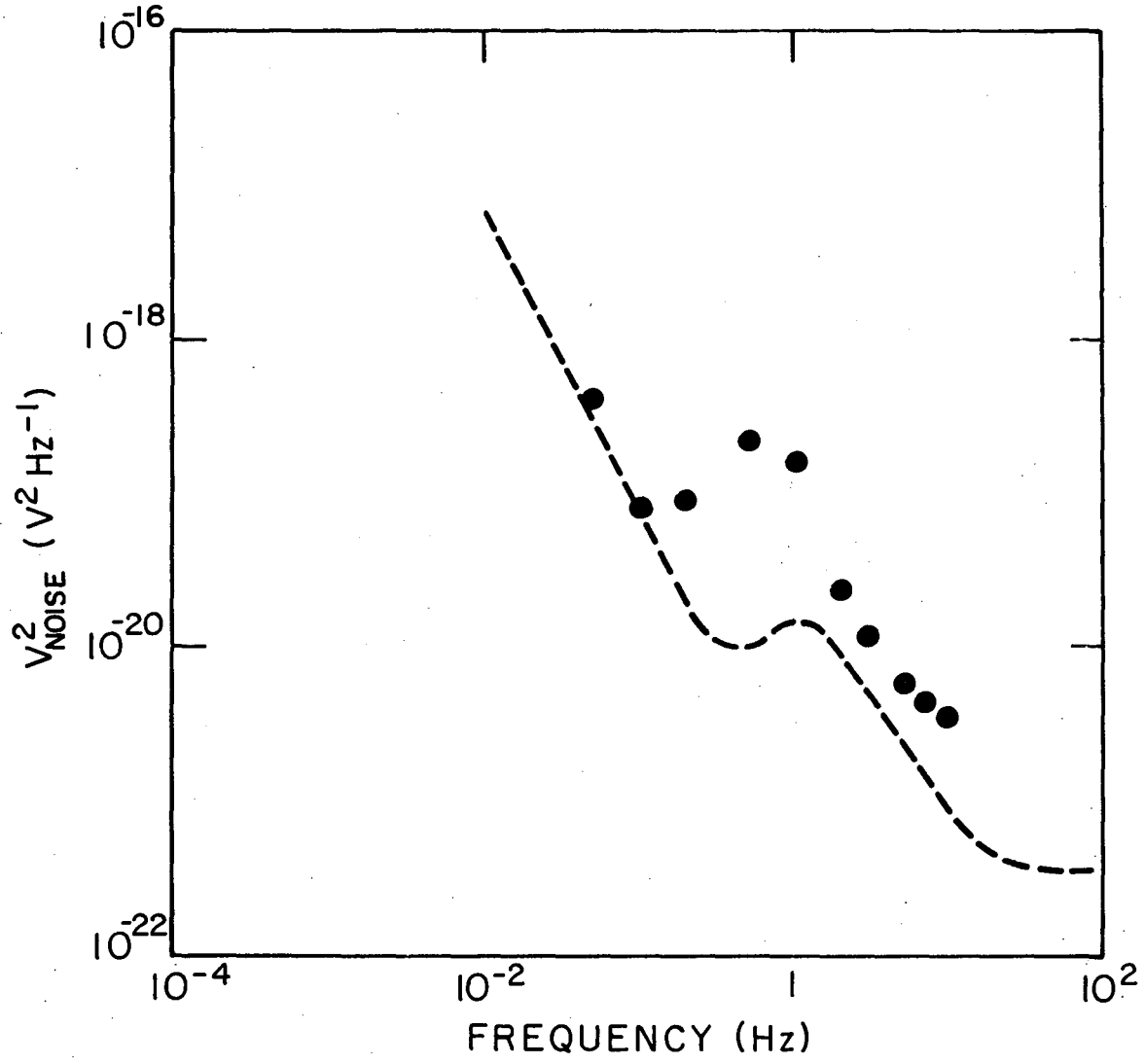
10^{-16}
10^{-18}
10^{-20}
10^{-22}
V^2_{NOISE} (V^2 Hz^{-1})
10^{-4}
10^{-2}
1
10^{2}
FREQUENCY (Hz)
XBL7612-7926

Fig. 5

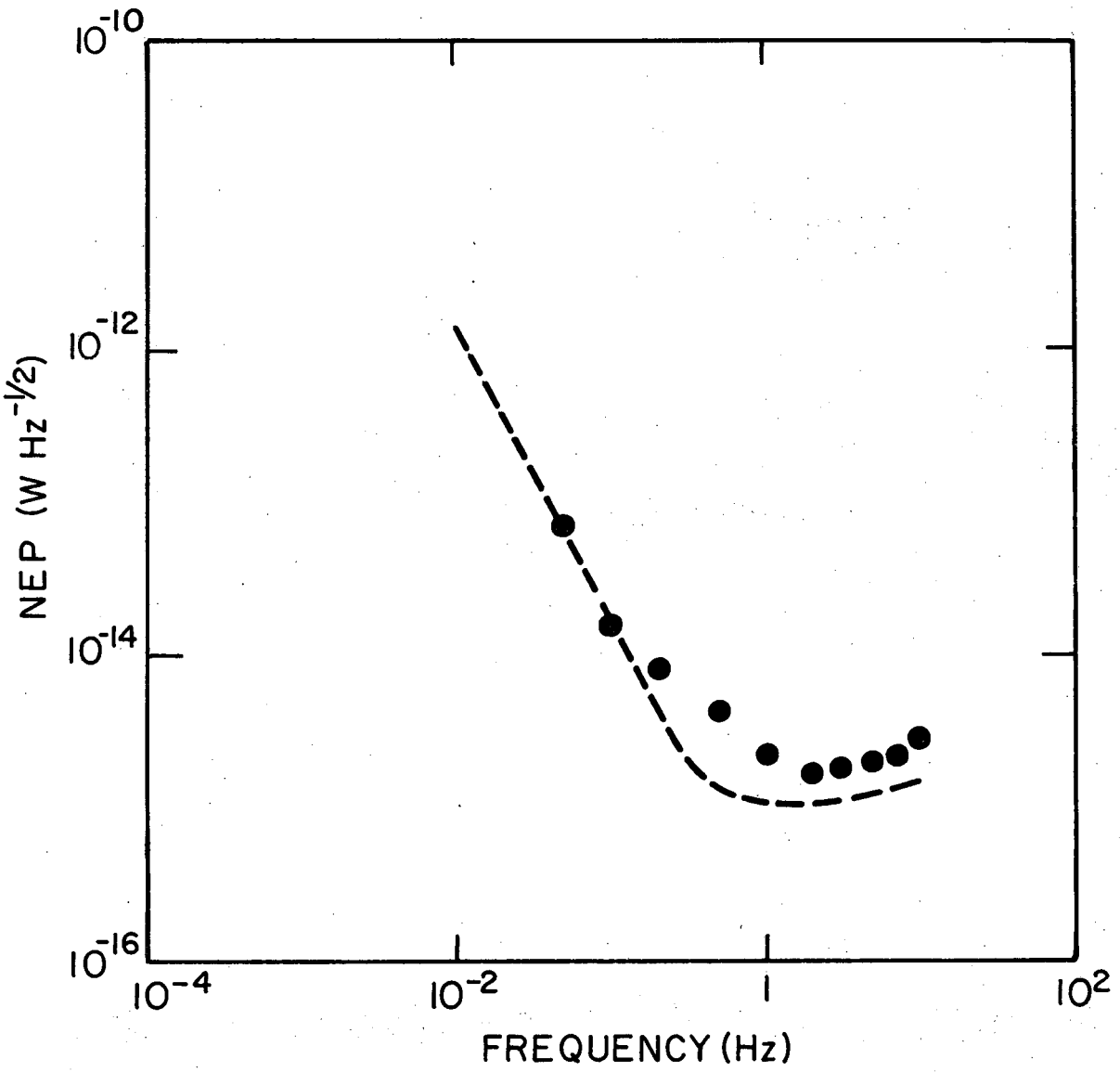

Fig. 6

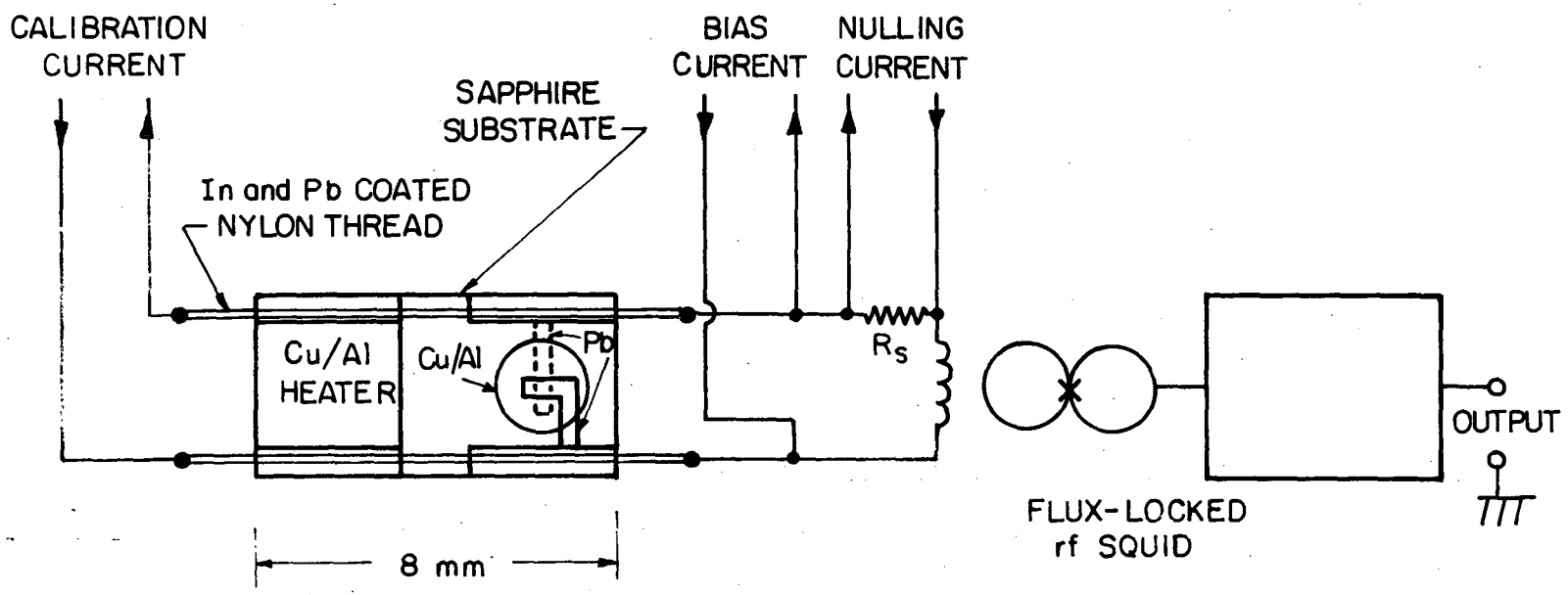

XBL771-4929

Fig. 7

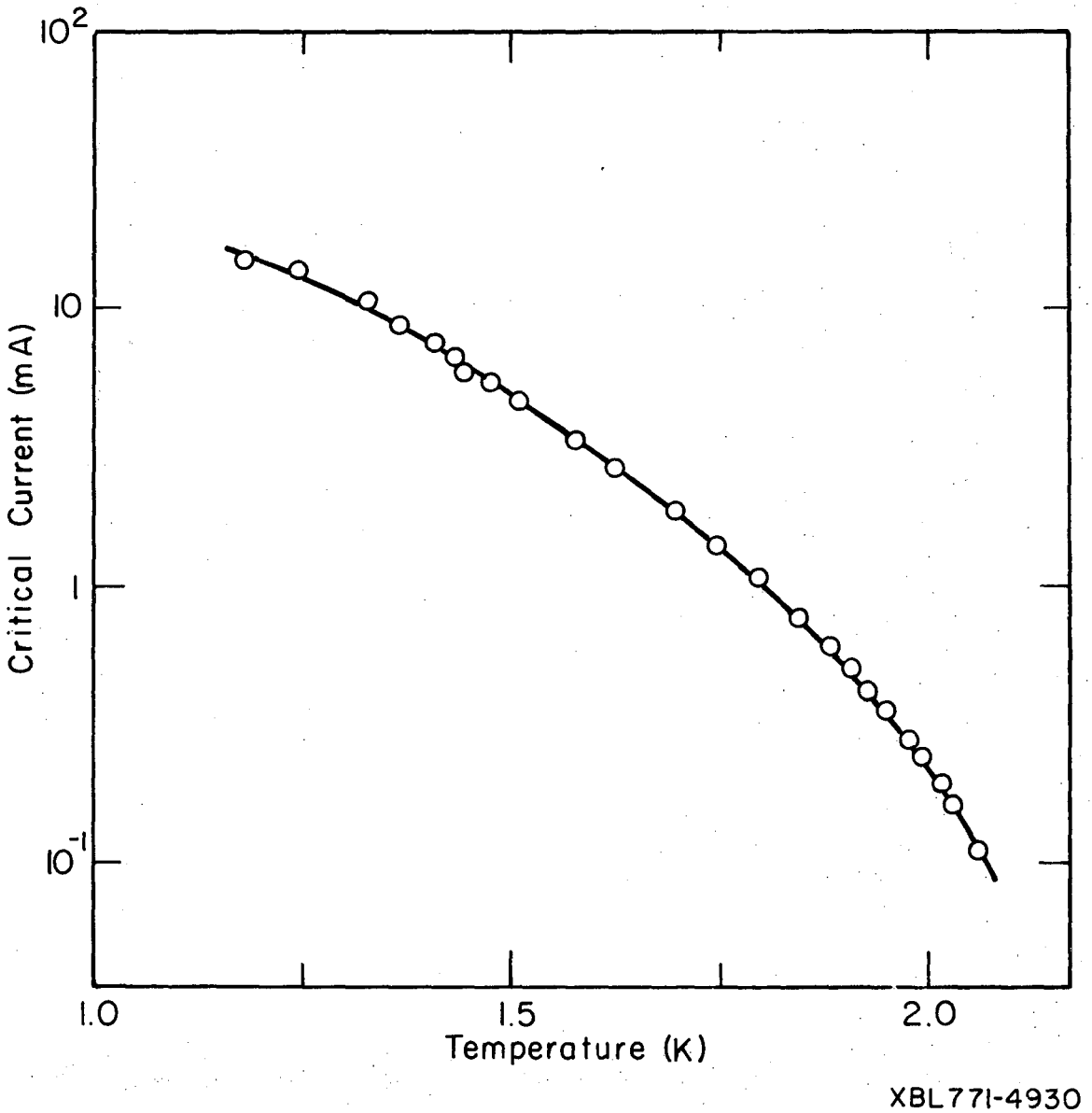

Fig. 8

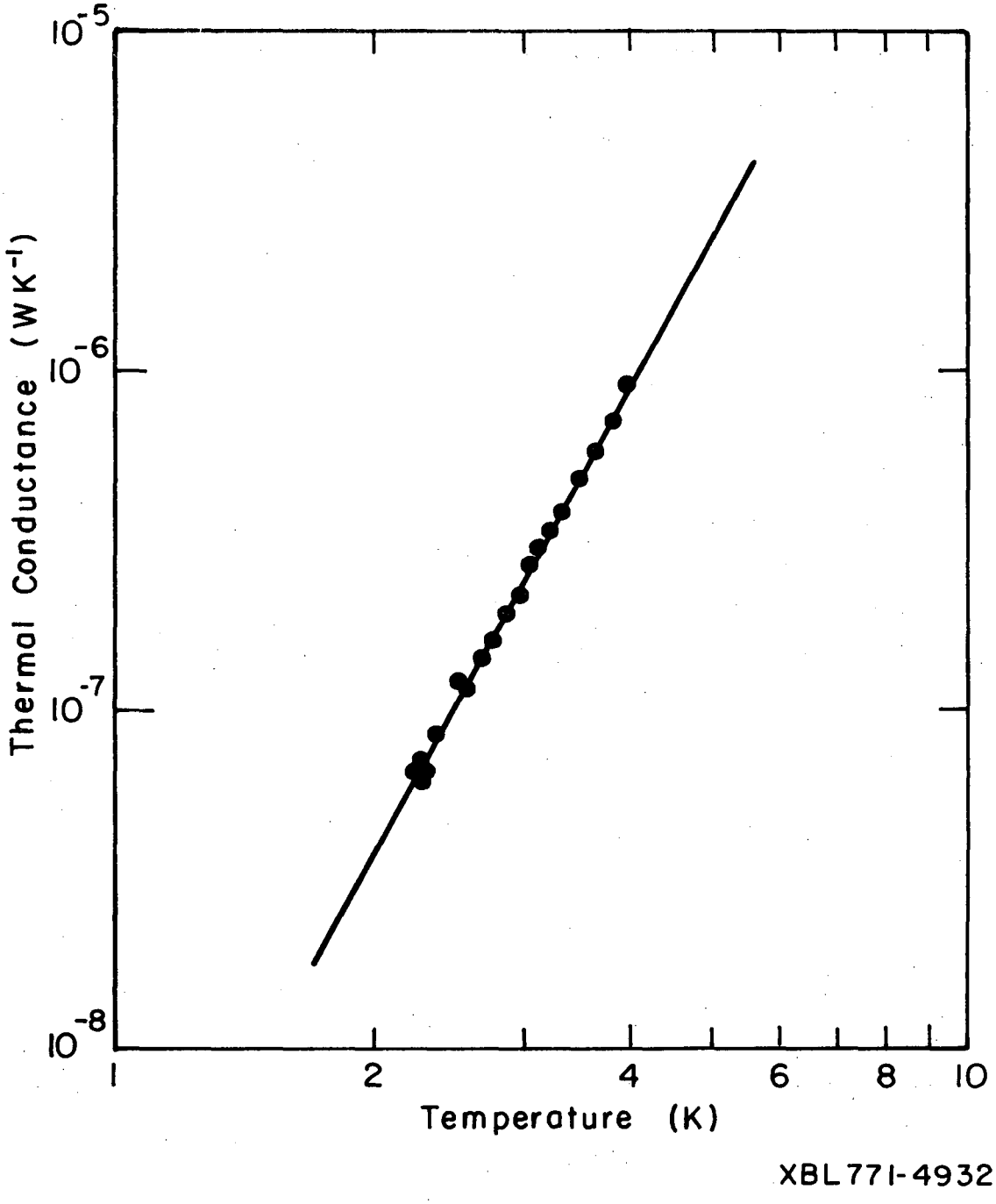
Thermal Conductance (WK⁻¹)
10⁻⁵
10⁻⁶
10⁻⁷
10⁻⁸
1
2
4
6
8
10
Temperature (K)
XBL771-4932

Fig. 9

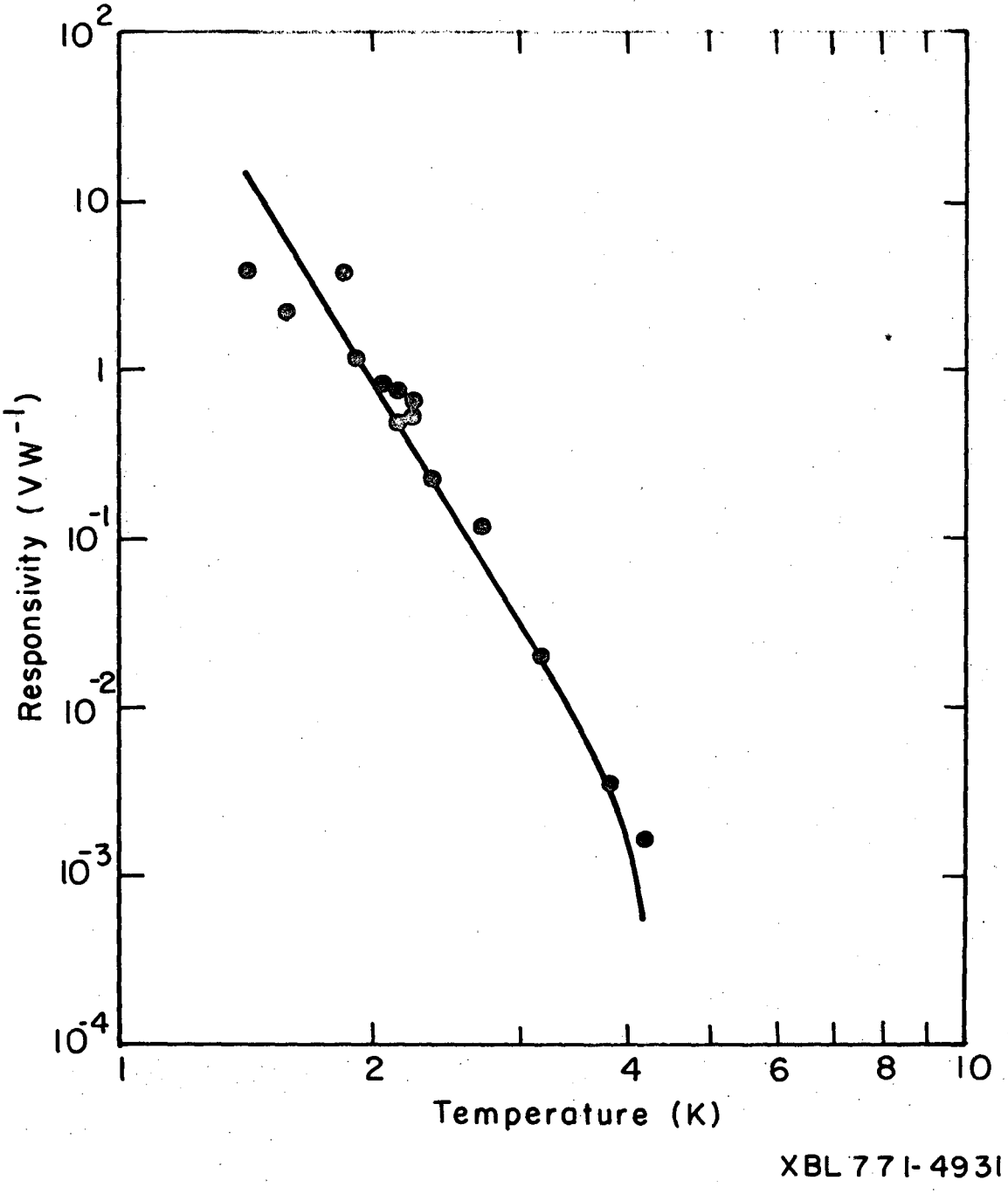

Fig. 10

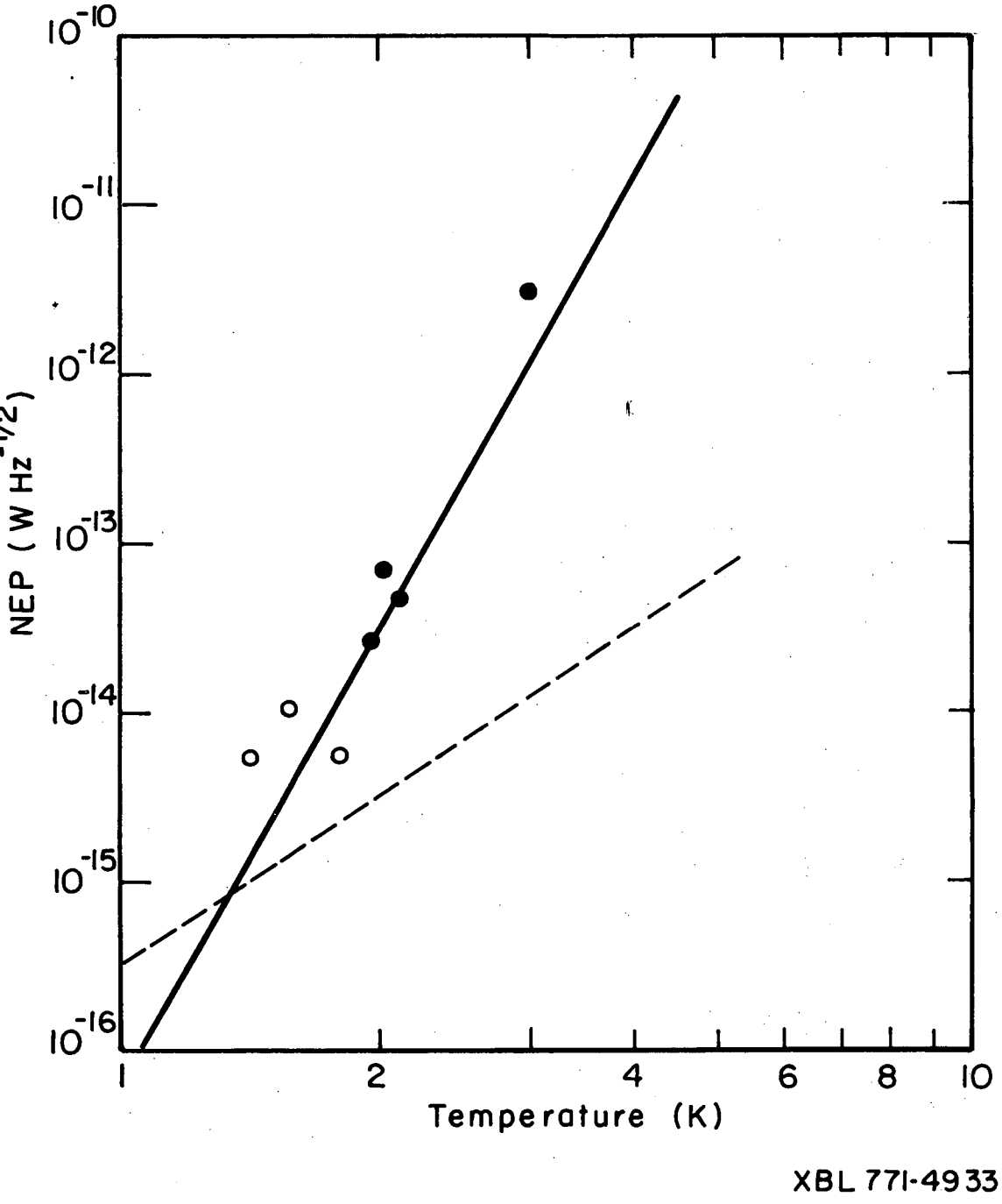
10^{-10}
10^{-11}
10^{-12}
10^{-13}
10^{-14}
10^{-15}
10^{-16}
NEP (W Hz$^{-1/2}$)
1
2
4
6
8
10
Temperature (K)
XBL 771-4933

Fig. 11

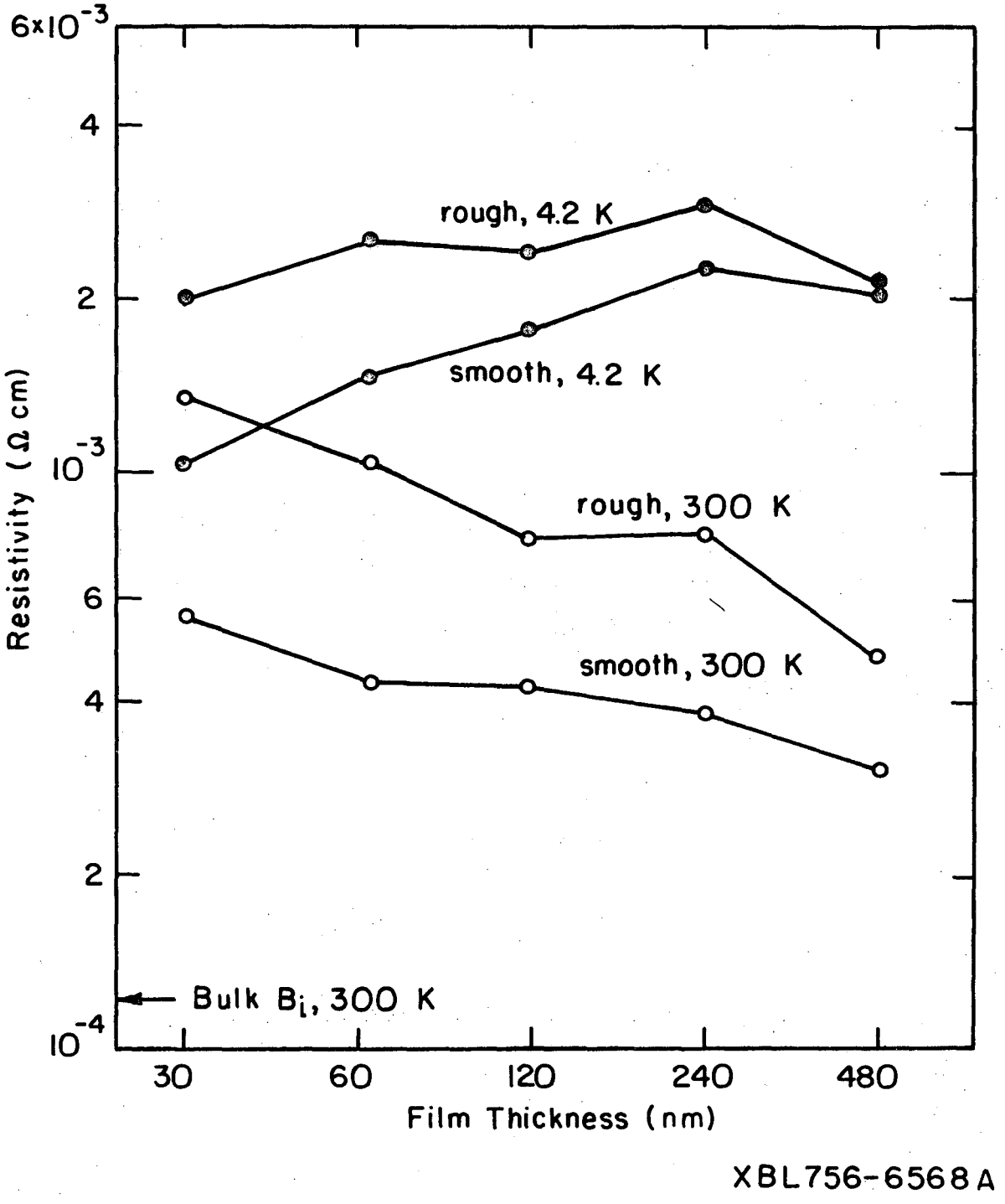
6x10^-3
4
2
10^-3
6
4
2
10^-4
Resistivity (Ω cm)
rough, 4.2 K
smooth, 4.2 K
rough, 300 K
smooth, 300 K
Bulk Bi, 300 K
30
60
120
240
480
Film Thickness (nm)
XBL756-6568A

Fig. 12

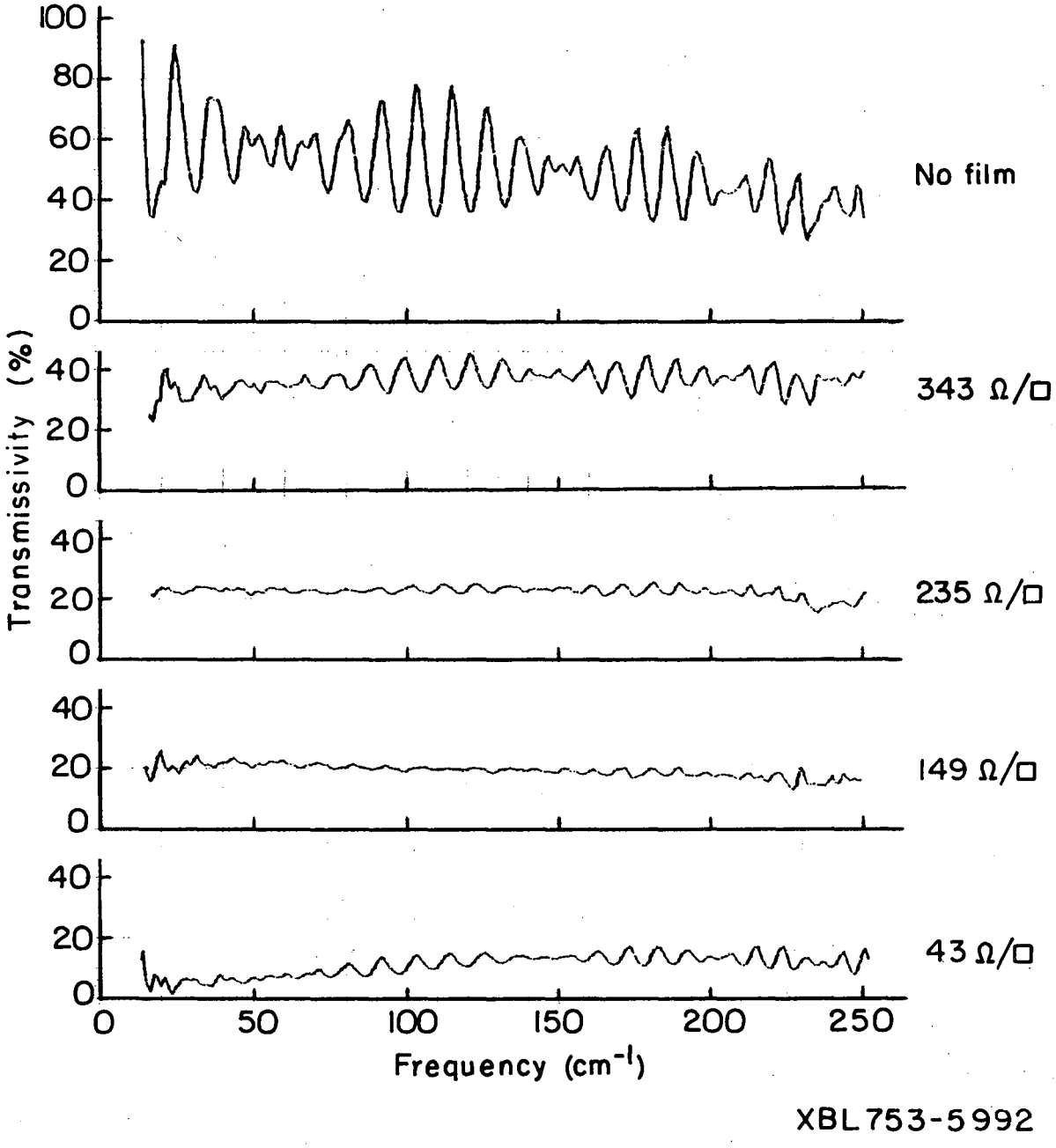
100
80
60
40
20
0
No film
Transmissivity (%)
40
20
0
343 Ω/□
40
20
0
235 Ω/□
40
20
0
149 Ω/□
40
20
0
43 Ω/□
0
50
100
150
200
250
Frequency (cm⁻¹)
XBL753-5992

Fig. 13

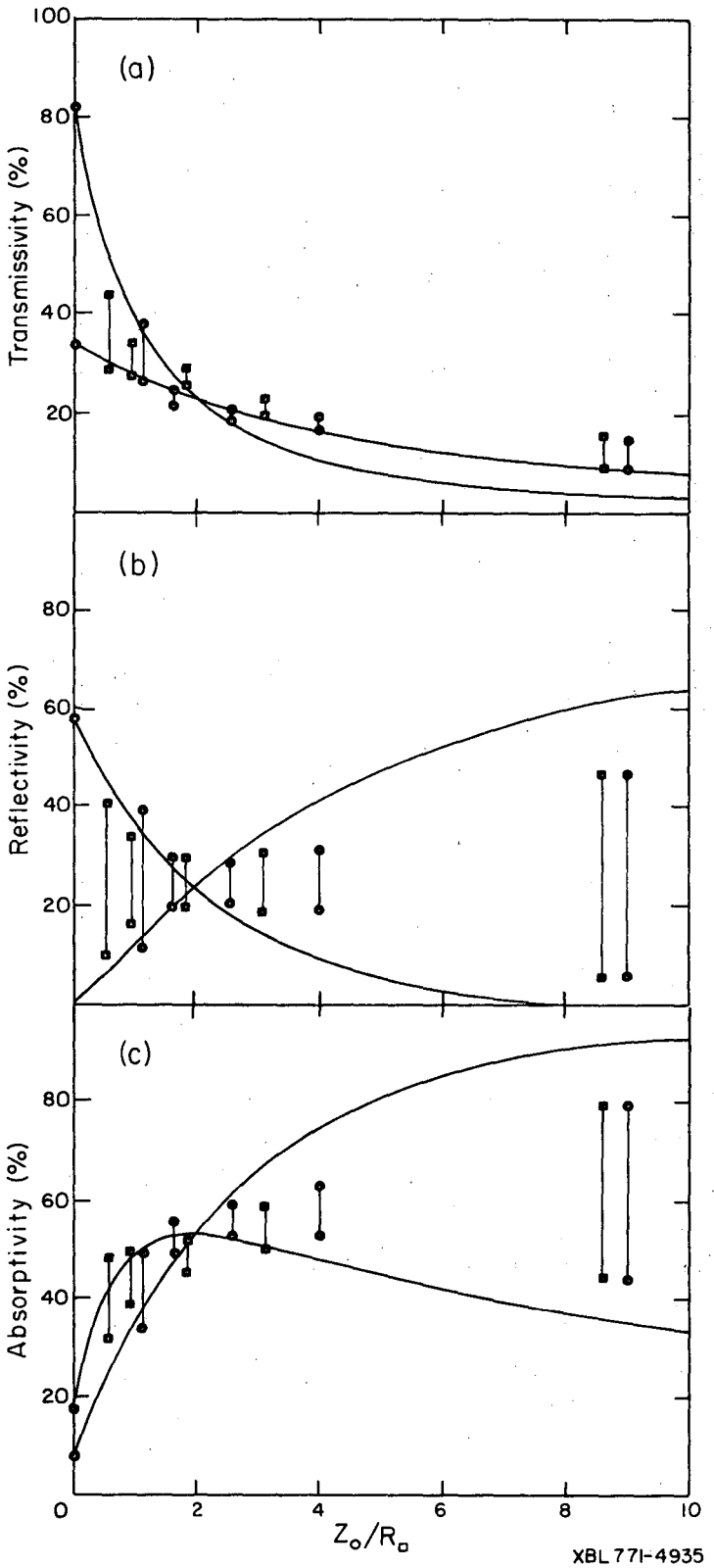

Fig. 14

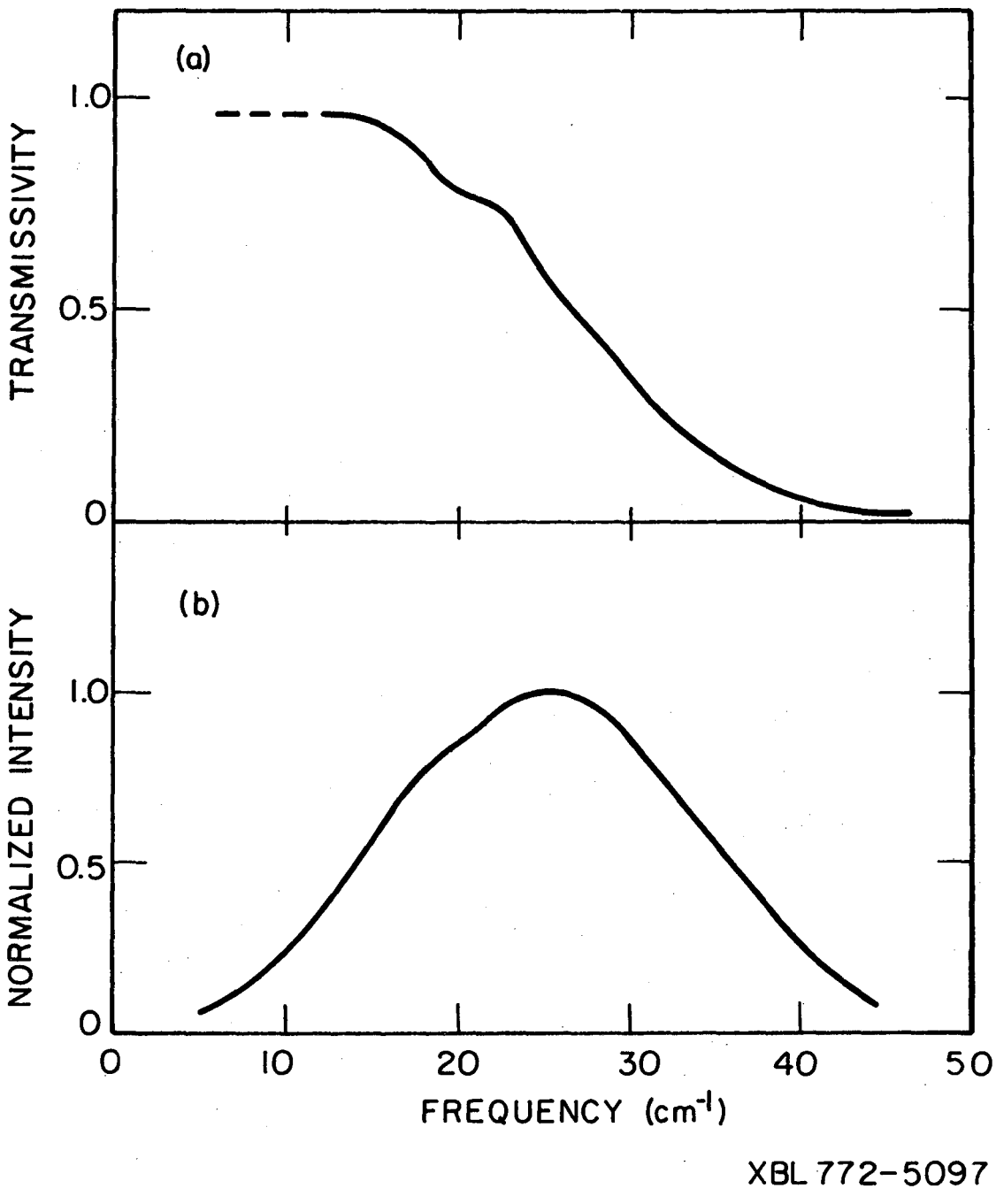
(a)
1.0
0.5
0
TRANSMISSIVITY
(b)
1.0
0.5
0
NORMALIZED INTENSITY
0
10
20
30
40
50
FREQUENCY (cm⁻¹)
XBL 772-5097

Fig. 15

TECHNICAL INFORMATION DIVISION
LAWRENCE BERKELEY LABORATORY
UNIVERSITY OF CALIFORNIA
BERKELEY, CALIFORNIA 94720